



Analysis and Design of ADSL
in
Enterprise Network

by

Sutud Jarupornprateep

Faculty of Engineering

October 2000

Analysis and Design of ADSL in Enterprise Networks

A thesis

submitted to the Faculty of Engineering

by

Sutud Jarupornprateep

in partial fulfillment of the requirements

for the degree of

Master of Engineering in Broadband Telecommunications

Advisor: Dr. Sudhiporn Patumtaewapibal

Assumption University

Bangkok, Thailand

October 2000

“Analysis and Design of ADSL in Enterprise Network”

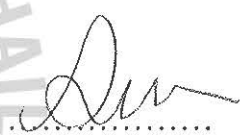
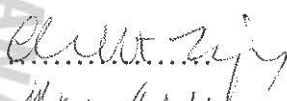
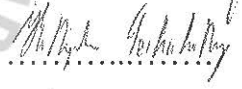
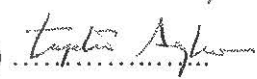
by

Mr.Sutud Jarupornprateep

A Thesis submitted in partial fulfillment
of the requirements for the degree of

Master of Engineering
Majoring in Broadband Telecommunications

Examination Committee:

- | | | |
|------------------------|------------------------------|---|
| 1. Dr.Sudhiporn | Patumtaewapibal (Advisor) |  |
| 2. Dr.Thiraphong | Charoenkhunwiwat (Member) |  |
| 3. Dr.Kittiphan | Techakittiroj (Member) |  |
| 4. Asst.Prof.Dr.Tuptim | Angkaew (MUA Representative) |  |

Examined on: October 27, 2000

Approved for Graduation on: ...December 22, 2000

Faculty of Engineering, Assumption University
Bangkok, Thailand

ABSTRACT

Asymmetrical Digital Subscriber Lines (ADSL) are developed to enhance the effectiveness of the existing telephone subscriber loops. Normally the loop plant connecting between the Central Office and the Customer Premise is very long and has only one or two bridge taps. ADSL for the enterprise system is different from the general ADSL systems in that the loop length is much shorter and it has many bridge taps than the normal ADSL telephone loop plant. Because of the wiring limitation for enterprise ADSL system so the low pass filter is developed to be used instead of POTS splitter for commercial purpose.

As the purpose of the thesis, the effect of the layout and bridge taps of the telephone loop plant to the data transmission bit rate capability of the enterprise ADSL system is investigated. The Discrete Multitone (DMT) signaling scheme is used to simulate the enterprise ADSL system. DMT downstream Far-End Crosstalk (FEXT), AWGN, and Near-End Crosstalk (NEXT) from DMT upstream are considered as the impairments. The simulation result shows that the effect of telephone loop is more severe than the effect of the number of bridge taps, and the maximum distance of the telephone loop with maximum data transfer rate of both upstream and downstream 1.2 km. This is also shown that ADSL can be applied to use in the hotel environment effectively.

ACKNOWLEDGEMENT

First thanks must go to my advisor Dr. Sudhiporn Patumtaewapibal, Dean of the Faculty of Engineer. His consistent advice, encouragement and confidence were essential for completion of this thesis. I am also very thankful to Dr. Thiraphong Charoenkhunwiwat for giving valuable advice and support everything.

Thank to Dr. Nick Marly, former Director of Broadband Telecommunications and Dr. Kittiphan Teachakittiroj, Acting Director of Broadband Telecommunications, for guiding and assisting me of making my thesis.

I also want to thank Mr. Jerapong Rojanarowan for helping of my design and giving advice. I am also grateful to all my other friends and colleagues at the department of Broadband Telecommunications. I could not have completed this master's degree thesis without the help of these people.

I wish to express my sincerest appreciation to my parents, who understand and support me to finish my study. Finally I wish to thank all the people who have made this work possible. Thank you.

TABLE OF CONTENTS

	Page
ABSTRACT	i
ACKNOWLEDGMENT	ii
TABLE OF CONTENTS	iii
LIST OF FIGURES	vi
LIST OF TABLES	ix
CHAPTER 1 INTRODUCTION	1
1.1 Background	1
1.2 Chapter Description	3
CHAPTER 2 ADSL BACKGROUND	5
2.1 Literature Review for in-house ADSL system	5
2.2 ADSL Overview	6
2.3 ADSL Capability	7
2.4 ADSL Technology	8
2.5 Standards and Associations	10
2.6 Twisted Pair Environment	10
2.6.1 Electrical Characteristics of Twisted Pair	10
2.6.2 Transmission Line Parameters	11
2.7 Crosstalk Types	11
2.8 DSL Theoretical Capacity	14
2.9 Basic DMT Description	15
2.9.1 DMT Implementation Basics	17
2.9.2 Constellation encoder	18
2.10 ADSL Frame Format	20

2.11 Forward Error Correction	23
2.12 Interleaving	23
2.13 Scrambling	24
2.14 Equalization	25
2.15 Shaping	26
CHAPTER 3 LOOP ANALYSIS	27
3.1 ABCD Parameters	27
3.2 Bridge Taps	30
3.3 Power Spectral Density	35
3.4 Disturbers	40
3.4.1 NEXT Disturbers	40
3.4.2 FEXT Disturbers	41
3.5 Performance Analysis	42
3.6 The SNR Gap	44
3.7 POTS Splitter	46
CHAPTER 4 ADSL IN THE HOTEL CASE STUDY	50
4.1 Low Pass Filter	51
4.2 Simulation and Measurement	53
4.2.1 Simulation	53
4.2.2 Measurement	62
4.2.3 Comparison	64
4.2.4 Recommendations	65
4.3 Cost Analysis	65
CHAPTER 5 CONCLUSION	67
APPENDIX A 22 and 24 AWG Characteristic	69

APPENDIX B Matlab's script features	73
APPENDIX C Component Price List	74
BIBLIOGRAPHY	75



LIST OF FIGURES

Figure	Page
2.1 ADSL system applications architecture	6
2.2 Basic ADSL Modem function	9
2.3 FDM and Echo Cancellation	9
2.4 Near-End Crosstalk (NEXT) and Far-End Crosstalk (FEXT)	12
2.5 ADSL transmission environment	13
2.6 DMT examples	16
2.7 Discrete Multi-Tone (DMT) Channelization	16
2.8 ATU-C transmitter block diagram	17
2.9 Constellation labels for $b = 2$ and $b = 4$	19
2.10 Constellation labels for $b = 3$ and $b = 5$	20
2.11 ADSL superframe data organization	22
3.1 A generic two port network	27
3.2 A twisted pair transmission line; the forward ($V_{x=L}^+$) and backward ($V_{x=L}^-$)	28
3.3 An equivalent two-port network for a twisted pair	28
3.4 A two-port network consisting of a lumped parallel impedance	30
3.5 A common bridged tap configuration on a twisted pair	31
3.6 A generic end-to-end model of the loop including generator and load impedance	33
3.7 Common method of producing an ADSL downstream signal	36
3.8 The effect of passing a signal through a linear, time-invariant filter on the signal's PSD	37
3.9 DMT ADSL downstream PSD	38

3.10	Common method of producing an ADSL upstream signal	39
3.11	DMT ADSL upstream PSD	40
3.12	NEXT PSD of 10 ADSL downstream	41
3.13	10 DMT ADSL FEXT disturbers on 24 AWG with 12,000 ft. loop	42
3.14	DMT decomposition of a transmission channel	42
3.15	Circuit Diagram of a POTS Splitter	47
3.16	Desired Lowpass and Highpass Frequency Responses for a POTS Splitter	47
4.1	Network of Sukhothai	50
4.2	ADSL in the access network	51
4.3	Purpose of splitter filter	51
4.4	Lowpass Filter Schematic	52
4.5	Frequency response of the Lowpass Filter	52
4.6	The characteristic impedance of the Low Pass Filter	53
4.7	Bridge tap detail for room 253	53
4.8	Bridge tap detail for room 556	54
4.9	Transfer function magnitude for room 253 (about 200 metres from Stinger)	56
4.10	Transfer function magnitude for room 556 (about 500 metres from Stinger)	56
4.11	Insertion Loss for room 253 (about 200 metres from Stinger)	57
4.12	Insertion Loss for room 556 (about 500 metres from Stinger)	57
4.13	SNR for room 253(downstream) with 24 DMT Downstream FEXT, 24 DMT Upstream NEXT and AWGN	58

4.14	SNR for room 253(upstream) with 24 DMT Upstream FEXT, 24 DMT Downstream NEXT and AWGN	58
4.15	SNR for room 556(downstream) with 24 DMT Downstream FEXT, 24 DMT Upstream NEXT and AWGN	59
4.16	SNR for room 556(upstream) with 24 DMT Downstream FEXT, 24 DMT Upstream NEXT and AWGN	59
4.17	SNR at distance of 2.3 km. with 24 DMT Downstream FEXT, 24 DMT Upstream NEXT and AWGN	61
4.18	SNR at distance of 1.2 km. with 24 DMT Upstream FEXT, 24 DMT Downstream NEXT and AWGN	61
4.19	Data rate versus loop length. Impairments are 24 DMT Downstream FEXT, 24 DMT Upstream NEXT and AWGN at -140 dBm/Hz	62
4.20	Downstream bit rate at Sukhothai Hotel	63
4.21	Upstream bit rate at Sukhothai Hotel	63
4.22	Ethernet frame format	64
4.23	ATM Transmission cell	64

LIST OF TABLES

Table	Page
2.1 ADSL Data Transmission Rate Standard	8
4.1 Simulation Parameters	55
A.1 22 AWG Characteristic at 70 Degrees F	69
A.2 24 AWG Characteristic at 70 Degrees F	71
C.1 Component Price List	74



CHAPTER 1. INTRODUCTION

1.1 Background

The ADSL (Asymmetric Digital Subscriber Lines) system was discovered by J. W. Lechleider in 1989 [14]. The ADSL system is utilized to support VOD (Video on Demand) system, high-speed video-based Internet Access, digital TV broadcasting, etc. The ADSL system can be implemented on the existing telephone infrastructure and the Plain Old Telephone Services (POTS). As the existing telephone infrastructure is used, the frequency of ADSL system has to be greater than 20 kHz to separate the voice band from ADSL system. Furthermore, the ADSL system can effectively work with ATM system, since the ADSL system has also been developed to support the random nature of data communication with Discrete Multitone (DMT) transmission method. The ADSL is a full duplex system by having the transmission speed of downstream faster than that of upstream. The downstream transmission is the transmission from the Central Office to Customer Premise, and the upstream transmission is the transmission from the Customer Premise back to Central Office. Nowadays, the ADSL system has become more and more popular with its major advantages of using the existing telephone infrastructure and providing much faster transmission speed than the other transmission method over normal telephone line.

As the ADSL system can achieve the very high speed information transmission through the telephone line, there is increasingly the idea of applying the ADSL system to use in a large building system. The hotel businesses are very interested in such an idea. By using the ADSL system, the hotel does not need to install the new wiring

network for the entire hotel area, because the ADSL system can be implemented on the existing telephone lines. This can reduce much of the cost, as the cost of installing the new wiring network is very expensive. Moreover, installing the new wiring network may interrupt the services given to customers causing the hotel cannot serve the customers effectively during the wiring installation. During the installation of the ADSL system, the hotel can provide continuous services to customers. Additionally, the hotel will be able to provide the high speed information transmission to customers by using the ADSL system.

Originally, the ADSL system is developed to support the connection between Central Office and Customer Premise by using Plain Old Telephone Services (POTS). The distance between Central Office and Customer Premise is quite far away, and there are only one or two bridge taps along the distance. These two parameters, distance and bridge tap, are different from the enterprise network, like the hotel. First, for the hotel network, the distance between Central Office and Customer Premise is the distance of telephone line connection from the control room to every room in the hotel. Therefore, the distance of the enterprise network is much shorter than the distance between Central Office and Customer Premise that uses in normal Plain Old Telephone Services. Second, for the hotel network, the amount of bridge taps needed for customer telephone service in every hotel room is very high. The hotel has to provide many telephone sets at different area of the room to serve customers. The amount of bridge taps varies according to the size of the room. In the large room, there will be the bridge taps for internal telephone service at 10 areas of the room to serve customers. In the small room, the bridge taps are needed for only 2 areas of each room.

The purpose of this thesis is to study the effect of the above mentioned two factors against the data transfer rate, and to study the potentiality of applying the ADSL system with the enterprise network, like the hotel for example.

1.2 Chapter Description

In Chapter 2, the basic knowledges of ADSL system, such as Discrete Multitone (DMT), Constellation Encoder Technique, ADSL Frame Format, and the disturbance that effect ADSL system, are provided for the preliminary understanding of ADSL system. In Chapter 3, the topic of Loop Analysis concerning transmission line is mentioned. The discussion mainly involves the effect of bridge taps to the Transfer Function and Insertion Loss of the transmission line. For the bridge taps in the transmission line, the concept of Two-Ports Networks is applied in order to find out the Transfer Function of each transmission line. This Chapter also discusses on the Power Spectral Density (PSD) of both the DMT Downstream and the DMT Upstream systems which are the standards of the ADSL system [25], and the Power Spectral Density of two major disturbance which are Near-End Crosstalk (NEXT) and Far-End Crosstalk (FEXT). The computed PSDs of both DMT Downstream and DMT Upstream are used for the simulation in order to know the transmission bit rate capability of the transmission line. In Chapter 4, all PSDs from Chapter 3 are simulated by Matlab software to get the various effects of the transmission line layout and the bridge taps in the hotel operation. The simulation result will also be compared with the actual result measured inside the hotel. Chapter 5 presents the summary and conclusions. In addition, recommendations for future work are also discussed. Introduction on RLCG parameters

for both 22 and 24 AWG, Matlab's script features and Component Price List are shown in Appendix A, B and C respectively. Appendix A and B are used for all simulations in Chapter 3 and Chapter 4. The component price list in Appendix C is used to estimate the total cost per room in the Cost Analysis part of Chapter 4 by using Lucent equipments.



CHAPTER 2. ADSL BACKGROUND

Asymmetric Digital Subscriber Lines (ADSL) deliver high-rate digital data over existing ordinary phone-lines. A new modulation technology called Discrete Multitone (DMT) allows the transmission of high speed data. ADSL facilitates the simultaneous use of normal telephone services, ISDN, and high speed data transmission, eg., video. DMT-based ADSL can be seen as the transition from existing copper-lines to the future optical fiber-cables. This makes ADSL economically interesting for the local telephone companies. The companies can offer customers high speed data services even before switching to fiber-optics.

2.1 Literature Review for enterprise ADSL system

The ADSL performance study [2], [3] with ADSL noise environment [6] are normally used for the Central Office to Customer Premise with the long loop length and assume to have only one or two bridge tap. The ADSL performance study for the enterprise's environment system is different from the ADSL system because the loop length will be much shorter and it has many bridge taps than the normal ADSL telephone loop plant. Wiring limitation is the main concern for enterprise system like hotel's environment.

2.2 ADSL Overview

Asymmetric Digital Subscriber Lines (ADSL), a new modem technology, converts existing twisted-pair telephone lines into access paths for multimedia and high speed data communications. ADSL transmits up to 8 Mbps to a subscriber, and as much as 640 kbps in both directions. ADSL can literally transform the existing public information network from one limited to voice, text and low resolution graphics to a powerful, ubiquitous system capable of bringing multimedia, including full motion video, to everyone's home as figure 2.1.

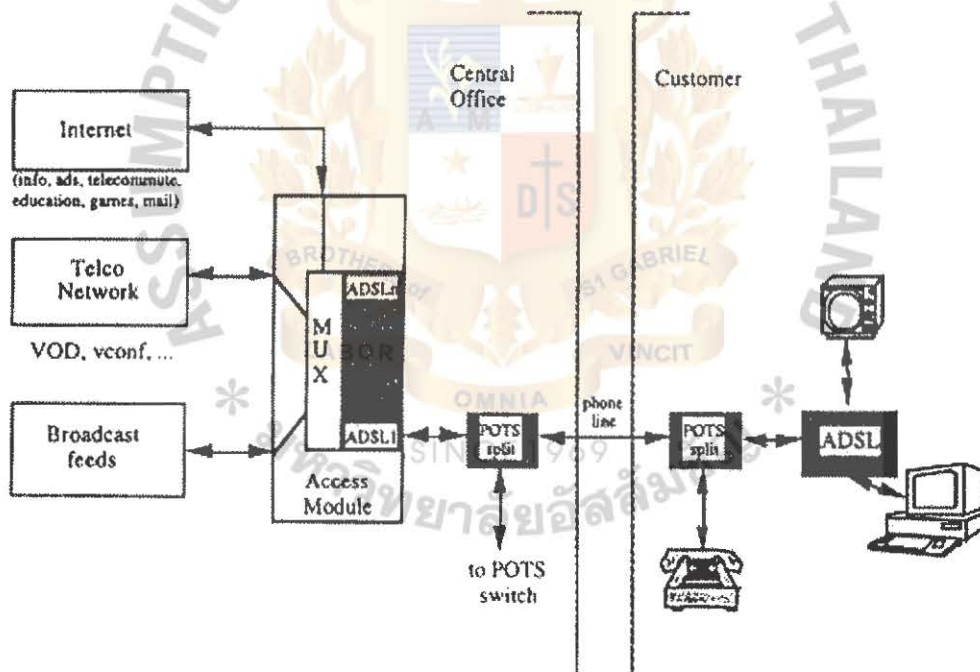


Figure 2.1 ADSL system applications architecture.

2.3 ADSL Capabilities

An ADSL circuit connects an ADSL modem on each end of a twisted-pair telephone line, creating three information channels - a high speed downstream channel, a medium speed duplex channel, depending on the implementation of the ADSL architecture, and a POTS (Plain Old Telephone Service) or an ISDN channel. The POTS/ISDN channel is split off from the digital modem by filters, thus guaranteeing uninterrupted POTS/ISDN, even if ADSL fail. The high speed channel ranges from 1.5 to 6.1 Mbps, while duplex rates range from 16 to 640 kbps [23]. Each channel can be submultiplexed to form multiple, lower rate channels, depending on the system. ADSL modem provide data rates consistent with North American and European digital hierarchies and can be purchased with various speed ranges and capabilities. The minimum configuration provides 1.5 or 2.0 Mbps downstream and a 16 kbps duplex channel; others provide rates of 6.1 Mbps and 64 kbps duplex. Products with downstream rates up to 8 Mbps and duplex rates up to 640 kbps are available today. ADSL modem will accommodate ATM transport layer with variable rates and compensation for ATM overhead, as well as IP protocols. Downstream data rates depend on a number of factors, including the length of the copper line, wire gauge, presence of bridge taps, and cross-coupled interference. Line attenuation increases when line length and frequency, and decreases as wire diameter increases. Ignoring bridge taps, ADSL will perform as follows [26]:

Data Rate	Wire Gauge	Distance	Wire Size	Distance
1.5 or 2 Mbps	24 AWG	18,000 ft	0.5 mm	5.5 km
1.5 or 2 Mbps	26 AWG	15,000 ft	0.4 mm	4.6 km
6.1 Mbps	24 AWG	12,000 ft	0.5 mm	3.7 km
6.1 Mbps	26 AWG	9,000 ft	0.4 mm	2.7 km

Table 2.1 ADSL Data Transmission Rate Standard.

2.4 ADSL Technology

ADSL depend upon advanced digital signal processing and creative algorithms to squeeze high information rate through twisted-pair telephone lines. In addition, many advances have been required in transformers, analog filters, and A/D converters. Long telephone lines may attenuate signals at one megahertz by as much as 90 dB [26], forcing analog sections of ADSL modem to work very hard to realize large dynamic ranges, separate channels, and maintain low noise figures. On the outside, ADSL look simple -- transparent synchronous data pipes at various data rates over ordinary telephone lines. On the inside, where all the transistors work, there is a miracle of modern technology.

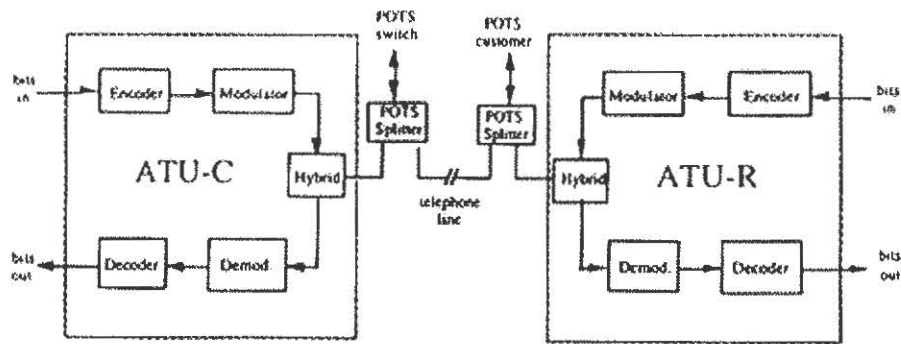


Figure 2.2 Basic ADSL Modem function.

The basic ADSL function is illustrated in figure 2.2. To create multiple channels, ADSL modem divide the available bandwidth of a telephone line in one of two ways -- Frequency Division Multiplexing (FDM) or Echo Cancellation as shown in figure 2.3. FDM assigns one band for upstream data and another band for downstream data. The downstream path is then divided by time division multiplexing into one or more high speed channels and one or more low speed channels. The upstream path is also multiplexed into corresponding low speed channels. Echo Cancellation assigns the upstream band to over-lap the downstream, and separates the two by means of local echo cancellation, a technique well known in V.32 and V.34 modems. With either technique, ADSL split off a 4 kHz region for POTS at the DC end of the band.



Figure 2.3 FDM and Echo Cancellation

2.5 Standards and Associations

The American National Standards Institute (ANSI), working group T1E1.4, recently approved an ADSL standard at rates up to 6.1 Mbps (ANSI Standard T1.413). The European Technical Standards Institute (ETSI) contributed an Annex to T1.413 to reflect European requirements. T1.413 currently embodies a single terminal interface at the premise end. Issue II will expand the standard to include a multiplexed interface at the premise end, protocols for configuration and network management, and other improvements. The ATM Forum and DAVIC (Digital Audio Visual Council) have both recognized ADSL as a physical layer transmission protocol for unshielded twisted pair media.

2.6 Twisted Pair Environment

2.6.1 Electrical Characteristics of Twisted Pair

For any transmission line, the basic parameters of interest are resistance, inductance, capacitance and admittance [12]. At frequency above the voice band, resistance, inductance and admittance vary with frequency. These three parameters also vary with gauge. Capacitance tends to be almost constant over both frequency and gauge (See Appendix A.)

2.6.2 Transmission Line Parameters

Two common parameters used, are the propagation constant (γ) and characteristic impedance ($Z_0(f)$), in characterizing voltage and current along the transmission line.

The propagation constant and characteristic impedance of any transmission line are defined in terms of the transmission line RLCG parameters, and are given by [18] as

$$\gamma = \alpha + j\beta = \sqrt{(R + j\omega L)(G + j\omega C)} \quad (2.6.2.1)$$

$$Z_0 = \sqrt{\frac{R + j\omega L}{G + j\omega C}} \quad (2.6.2.2)$$

where R is resistance, L is inductance, C is Capacitance, and G is admittance. If the transmission line is perfectly terminated with length d , the transfer function, $H(f)$, given in [5] is

$$H(f) = e^{-\alpha d} e^{-j\beta d} = |e^{-\alpha d}| \angle \beta d \quad (2.6.2.3)$$

where α and β are the real and imaginary parts of the propagation constant respectively.

2.7 Crosstalk Types

Crosstalk is generally characterized as either Near-End Crosstalk (NEXT) or Far-End Crosstalk (FEXT) as shown in figure 2.4.

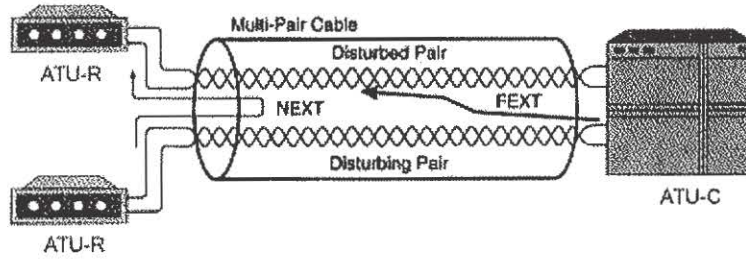


Figure 2.4 Near-End Crosstalk (NEXT) and Far-End Crosstalk (FEXT)

From figure 2.4, NEXT arises at the ATU-R when other ATU-R's upstream transmitted signals couple electromagnetically into the first ATU-R's signal, reverse direction, and thereby enter the first ATU-R's receiver. NEXT can also occur at the ATU-C end. NEXT coupling can be highly dependent on loop geometry and cabling practices, but a 1% worst-case approximation, used almost universally, is that the NEXT noise has a power spectrum given in [6] as follow

$$S_{NEXT}(f) = K_{NEXT} \cdot f^{3/2} \cdot S_X(f) \quad (2.7.1)$$

$$K_{NEXT} = 0.882 \times 10^{-14} \cdot N^{0.6} \quad (2.7.2)$$

where S_{NEXT} is a power spectrum of NEXT, K_{NEXT} is constant, N is the number of disturbers, f is frequency, and $S_X(f)$ is the power spectrum of the crosstalker's transmitted signal.

FEXT arises when other ATU-C's transmitted signals electromagnetically couple into the line and then traverse the line along with the intended signals to the ATU-R. The noise power spectrum of FEXT given in [6] is

$$S_{FEXT}(f) = K_{FEXT} \cdot f^2 \cdot d \cdot S_x(f) \quad (2.7.3)$$

where S_{FEXT} is a power spectrum of FEXT, K_{FEXT} is coupling constant varying on the number of disturbers, d is the distance in feet, and $S_x(f)$ is the ATU-C transmitted spectrum. The ADSL transmission environment is illustrated in figure 2.5. Disturbing signal due to NEXT usually has to travel over less length of the twisted pair before entering a disturbed pair's receiver as compared to FEXT. For this reason, NEXT from a particular disturber is usually more damaging than FEXT. AM radio signals can couple into phone lines, depending on the orientation of the line. AM radio signals are typically 10 kHz wide and can couple into phone lines leaving differential peak voltages of a few hundred millivolts [11]. Impulse noise is temporary disturbances, typically measuring between microvolts and tens of millivolts [16]. Impulse noise can be caused by everything from telephone company switch transients to refrigerators and light switches in the home.

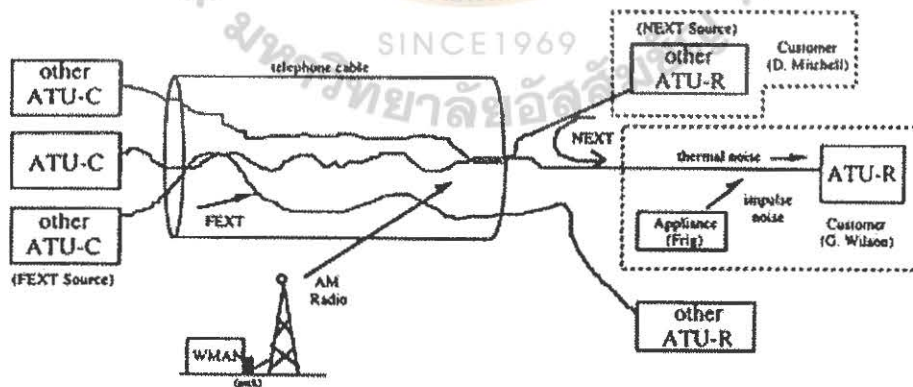


Figure 2.5 ADSL transmission environment.

2.8 DSL Theoretical Capacity

Both of loss on the twisted pair channel and crosstalk coupling between 2 twisted pairs are factors in determining the amount of information that a twisted pair channel can reliably carry [2]. Simply put, these factors determine the data rate capability of the twisted pair. The twisted pair channels with more loss support lower data rates than do twisted pairs with less loss. Similarly, a twisted pair with more crosstalk disturbance supports a lower data rate than a twisted pair with little or no crosstalk. Mathematically bounding channel capacity provides a benchmark for the performance of various types of coding and modulation techniques. For a continuous time channel, capacity is a function of signal power and noise power at the receiver of the channel. If a specific application uses only a certain frequency band on the channel, the frequency band used also affects capacity. Thus the SNR for the channel i at receiver is given by [19],

$$SNR_i = \frac{|G_i|^2 S_i}{|H_i Q_i + Z_i|^2} \quad (2.8.1)$$

In equation (2.8.1), S_i is the signal power for subchannel i at the transmitter. $|G_i|$ is the magnitude of the transfer function of subchannel i . H_i is the transfer function for disturber on subchannel i . Q_i is the signal power from a disturber for subchannel i . Z_i is the background additive white gaussian noise (AWGN) on a subchannel i . The total maximum rate of all channels is given in [19] as

$$R_{\max} = \sum_{i=1}^L \frac{B}{L} \log_2 \left(1 + \frac{|G_i|^2 S_i}{|H_i Q_i + Z_i|^2} \right) \quad (2.8.2)$$

where the original channel bandwidth is B Hz and L is the number of subchannels, then each subchannel will have a bandwidth of B/L Hz

2.9 Basic DMT Description

ANSI standard [1] describes a basic ADSL system which uses DMT (Discrete Multitone) modulation. DMT inherently transmits an optimized time-variable spectrum. This spectrum is adjusted according to the desired data rate and the transmission characteristics on each and every channel. The basic concept of DMT is illustrated by three examples in figure 2.6. In each case, DMT initialized by the ATU-C transmit 256 4-kHz-wide tones downstream. The ATU-R measures the quality of each of these tones and then decides whether a tone has sufficient quality to be used for further transmission and, if so, how much data this tone should carry relative to the other tones that are used. This procedure maximizes transmission performance. The degree of high-frequency attenuation depends on the length of the phone line: longer lines have greater attenuation [24].

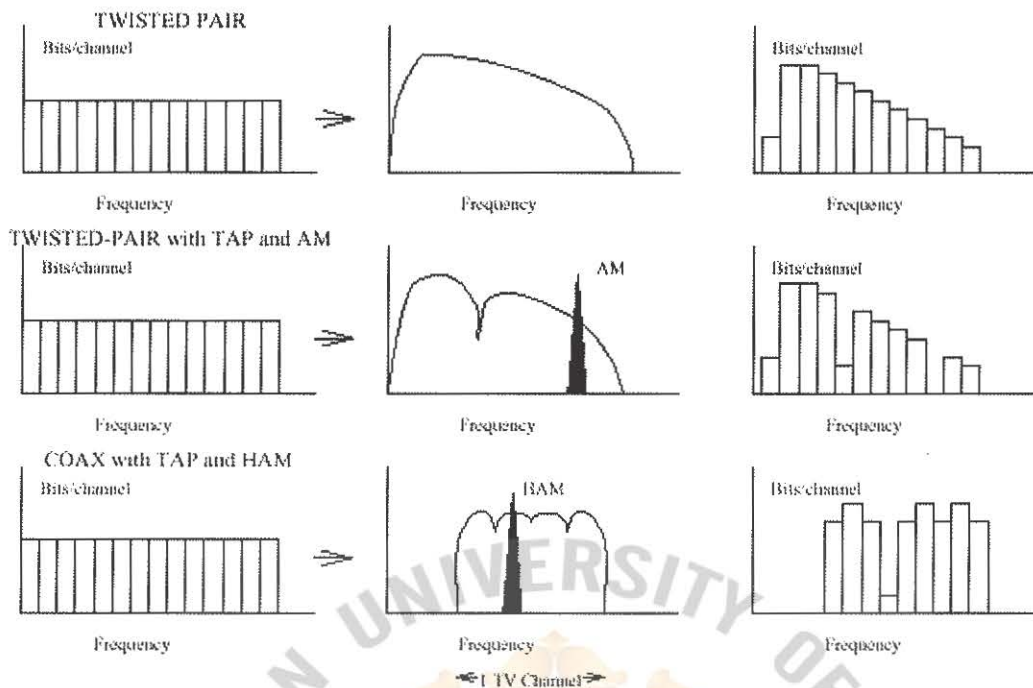


Figure 2.6 DMT examples.

In ADSL DMT systems the downstream bandwidth are divided into 250 4-kHz-wide tones and upstream bandwidth are divided into 26 subchannels, as indicated in figure 2.7 [13].

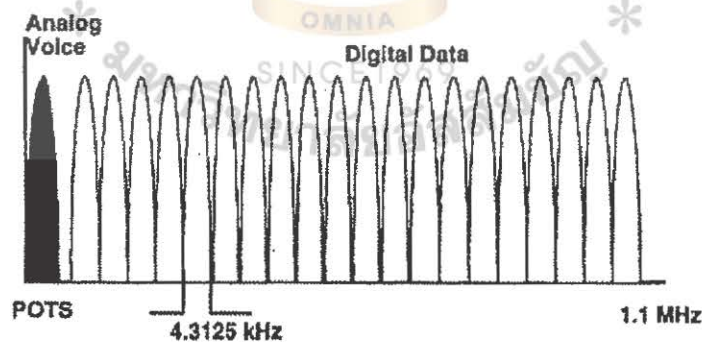


Figure 2.7 Discrete Multi-Tone (DMT) Channelization.

2.9.1 DMT Implementation Basics

The basic DMT implementation of the ATU-C transmitter for ADSL is given in figure 2.8. The incoming bits are coded in the ADSL standard through the use of forward-error-correction (FEC) coded, which appends extra bits to the original bit stream, and optionally the use of trellis coding [8].

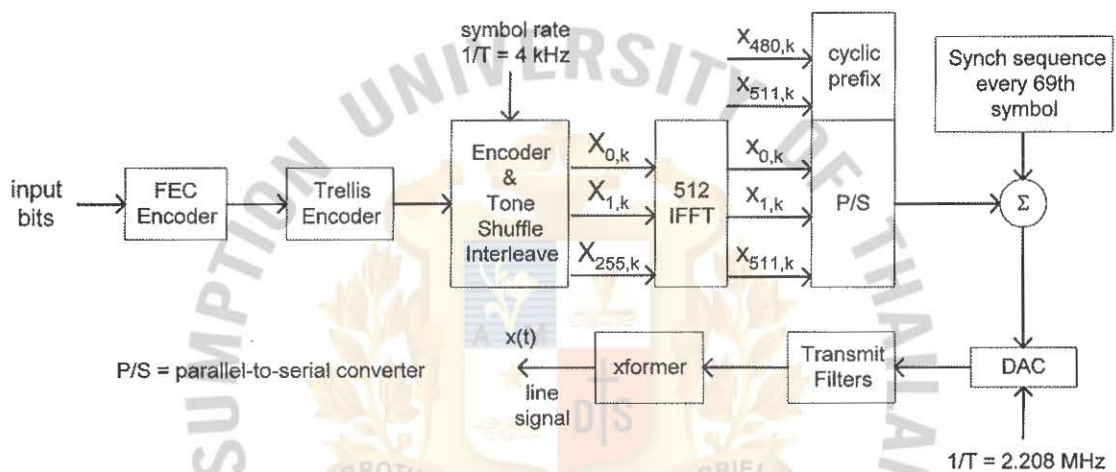


Figure 2.8 ATU-C transmitter block diagram.

The encoded bit parse into groups of b_i bits, $i = 0, \dots, 255$ bins or tones, for each tone at the output of the Trellis encoder. The result of the grouping is a two dimension quantity, X_i , that consists of a real part and an imaginary part. There are 2^{b_i} such complex values for i th tone, one to represent each of the 2^{b_i} input bit patterns for that tone. The process of encoding repeats for each of these 256 subchannels 4000 times per second. The loading process also determines the amount of energy applied to each tone. An IFFT of size 512 (complex to real) converts the complex sample ($X_i = X_{512-i}^*$, $i = 0, \dots, 255$) [25] into a real sequence of 512 samples x_k . The sequence represents the sum of modulated sinusoids. The formula for the IFFT is

$$x_k = \frac{1}{\sqrt{512}} \sum_{n=0}^{511} X_n e^{j \frac{\pi}{256} kn} \quad (2.9.1.1)$$

This prefix is the same value as the first 32 samples of the 512-sample sequence. The 512-sample sequence is then concatenate with 32 samples, so called cyclic prefix. For reliability, a dummy known synchronization symbol of 544 samples is inserted every 69th symbol, so that the aggregate sampling rate of the ATU-C transmitter is thus (544)(4000)(69/68) = 2.208 MHz. The upstream path is identical, except that the 512 IFFT is replaced by a 64 IFFT, with prepending of 32/8 = 4 samples, for an upstream sampling rate of 276 kHz so the formula for the IFFT of the ATU-R is

$$x_k = \frac{1}{\sqrt{64}} \sum_{n=0}^{63} X_n e^{j \frac{\pi}{32} kn} \quad (2.9.1.2)$$

The demodulator in an ADSL receiver very much follows from the modulator. AT the ATU-R, the heart of the modulator is basically an FFT operating on 512 real-valued points. Note that before the FFT is performed, the 32-sample cyclic prefix is removed. After FFT is performed, only the lower 256 complex FFT outputs are kept, and the other 256, which are complex conjugates, are dropped.

2.9.2 Constellation encoder

For a given sub-channel, the encoder selects an odd point (X,Y) from the square-grid constellation based on the b bits $v_{b-1}, v_{b-2}, \dots, v_1, v_0$. For convenience of description, these b bits are identified with an integer label whose binary representation is $(v_{b-1}, v_{b-2}, \dots, v_1, v_0)$. For example, for $b = 2$, the four constellation points are labeled 0, 1, 2, 3

corresponding to $(v_1, v_0) = (0,0), (0,1), (1,0), (1,1)$ respectively. The constellations for even values of b are shown in figure 2.9. The 4-bit constellation can be obtained from the 2-bit constellation by replacing each label n by the 2x2 block of labels [19]:

$$\begin{matrix} 4n + 1 & 4n + 3 \\ 4n & 4n + 2 \end{matrix}$$

The same procedure can be used to construct the larger even-bit constellations recursively.

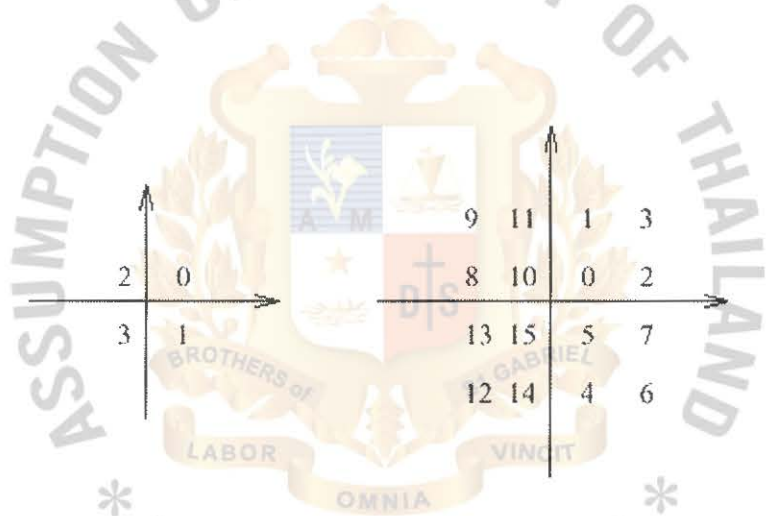


Figure 2.9 Constellation labels for $b = 2$ and $b = 4$

If b is odd and greater than 3, the 2 MSBs of X and the 2 MSBs of Y are determined by the 5 MSBs of the b bits. The constellations for odd values of b are shown in figure 2.10. The 5-bit constellation can be obtained from the 3-bit constellation by replacing each label n by the 2x2 block labels [5]:

$$\begin{matrix} 4n + 1 & 4n + 3 \\ 4n & 4n + 2 \end{matrix}$$

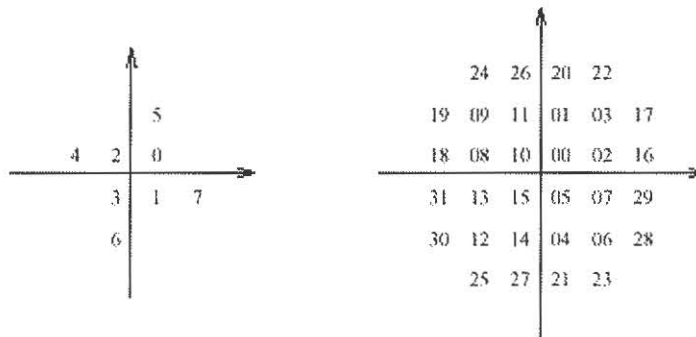


Figure 2.10 Constellation labels for $b = 3$ and $b = 5$

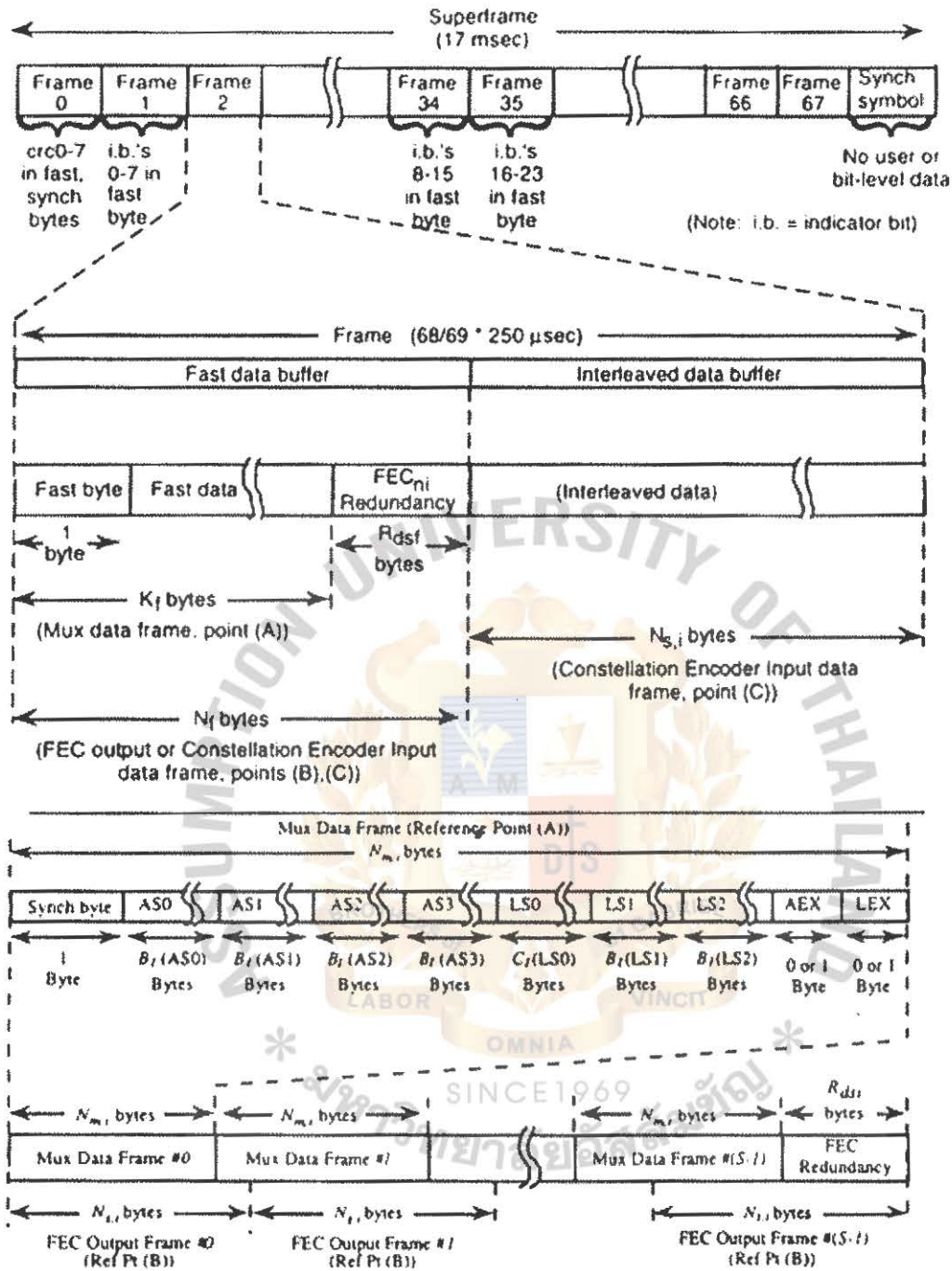
2.10 ADSL Frame Format

The ADSL superframe appears in figure 2.11 where 68 data-carrying packets are followed by a 69th synch symbol. The synch symbol is a known fixed repeated pattern, a DMT tone where most of the tones are transmitted and contain 2^b per tone from a pseudorandom pattern. This symbol can be used for quick recovery of frame alignment if lost because of a substantial interruption, like a few-second line outage. This symbol can also be used to derive timing phase. Shorter interruptions typically do not result in loss of frame with well-designed DMT receivers [8].

Each of the 68 symbols within the superframe has a length that is determined by the data rate and fast interleaving rate negotiation of ADSL. Within each symbol fast path data occurs first with a control byte known as the fast byte followed by the bytes of fast data and the corresponding parity bytes. Fast path codewords are never longer than one DMT symbol to keep latency to a minimum. The fast data is followed by the interleave data. The interleave data is also preceded by a control byte known as the synchronization

byte in each symbol. Because many DMT symbols may correspond to a codeword in the interleave path, the parity bytes are deferred until all information bytes have occurred. Within the data portions of either the fast or interleave sections of a symbol, the data corresponding to AS0, AS1, AS2, AS3, LS0, LS1, and LS2 occur in order. Any one of these must be in either the fast buffer or the interleave buffer. If unused, then there is zero byte for the unused ASX or LSX channel. Control bits in the fast and synch bytes allow the addition of a byte (AEX or LEX) to the information stream, or deletion of a byte. This add/delete mechanism allows the various application signals to be asynchronous, as is commonly encountered in ADSL serving multiple applications.

Whereas the frame structure of ADSL is conceptually complicated, the implementation in very large-size integration (VLSI) is negligible in gate count. Further, this highly flexible format has begun to prove itself as anticipating the varied uses of ADSL for multiple signals that are now beginning to occur. (In other words, the initial superframe structure had to be flexible because the applications that would drive ADSL use can not be accurately described.)



$$N_{m,i} = 1 + \sum_{j=0}^3 B_f(AS_j) + A_f + \sum_{j=0}^2 B_f(LS_j) + L_f$$

$$\text{where } A_f = \begin{cases} 0, & \sum_{j=0}^3 B_f(AS_j) = 0 \\ 1 & \text{otherwise} \end{cases}$$

$$\text{and } L_f = \begin{cases} 0, & \sum_{j=0}^3 B_f(AS_j) = \sum_{j=0}^2 B_f(LS_j) = 0 \\ 1 & \text{otherwise} \end{cases}$$

(Note: $L_f = 1$ when $B_f(LS_0) = 255$)

$$C_f(LS_0) = \begin{cases} 0, & B_f(LS_0) = 255 \text{ (Binary 11111111)} \\ B_f(LS_0) & \text{otherwise} \end{cases}$$

$$N_{s,i} = (S * N_{m,i} + R_{dsf}) / S,$$

where R_{dsf} = # FEC redundancy bytes
and S = # DMT symbols per FEC codeword

Figure 2.11 ADSL superframe data organization

2.11 Forward Error Correction

A forward error correction (FEC) block adds redundancy to the data to be transmitted. Usually this redundancy is a small fraction of the actual transmitted payload. The value of adding the redundancy is that the FEC block might be able to correct bits that the demodulator decodes incorrectly. The power of a forward error correction technique is often described using the term coding gain. A reasonable coding gain for a DSL forward error correction technique may be 3 dB at a bit error rate (BER) of 10^{-7} [17]. Stated another way, adding the FEC to the system makes the system perform as well as a system without coding but with twice the transmit power (3 dB more transmit power). This attribute is indeed formidable.

There are two common types of forward error correction in DSL systems. The first type is a cyclic block code known as a Reed-Solomon coding. The second one is a convolution code known as trellis-coded modulation (TCM) and ties in tightly with the constellation encoding used in both CAP/QAM and DMT modulation.

2.12 Interleaving

Many FEC blocks have trouble when it comes to correcting long strings of errors. Such errors are common on channels and can occur on DSLs (for example, when a transient spike is incident upon the twisted pair). The purpose of interleaving is to spread out a codeword such that channel burst errors are also spread out. Interleaving often occurs between a block forward error correction module and a modulation module in a

transmitter. The corresponding block in the receiver is a "de-interleaving" block. There are two types of interleavers: a block interleaver and a convolutional interleaver. Block interleavers are simple and easy to understand; however, convolutional interleavers are more common in DSLs, as they have delay and memory requirement advantages [19].

2.13 Scrambling

Most DSLs include a scrambler in the transmitter and a descrambler in the receiver. A scrambler decreases the probability that a long string of ones or zeros are passed to the modulator. Such strings may occur in either a packet-based system or an ATM system when no packets or cells exist to transmit and the input to the transmitter is held either high or low. Often it is said that a scrambler randomizes data and a descrambler removes the randomness. Scrambling has two positive benefits in a communications system. First, it helps ensure that the transmitted power spectral density observed at the output of the transmitter is predictable. When deriving equations for Power Spectral Density (PSD) an assumption was made about the statistics of the transmitter. Scrambling helps to make such assumptions valid.

Second, many types of circuits or algorithms depend on a mix of ones and zeros to operate properly. Timing recovery phase locked loops and some adaptive equalization algorithms are good examples of these. Scrambling helps ensure that such blocks function properly. Note that scrambling in a transmitter is typically not used for data

encryption or security purposes. The means of descrambling received data at the receiver are much too simple to be effective for security applications.

2.14 Equalization

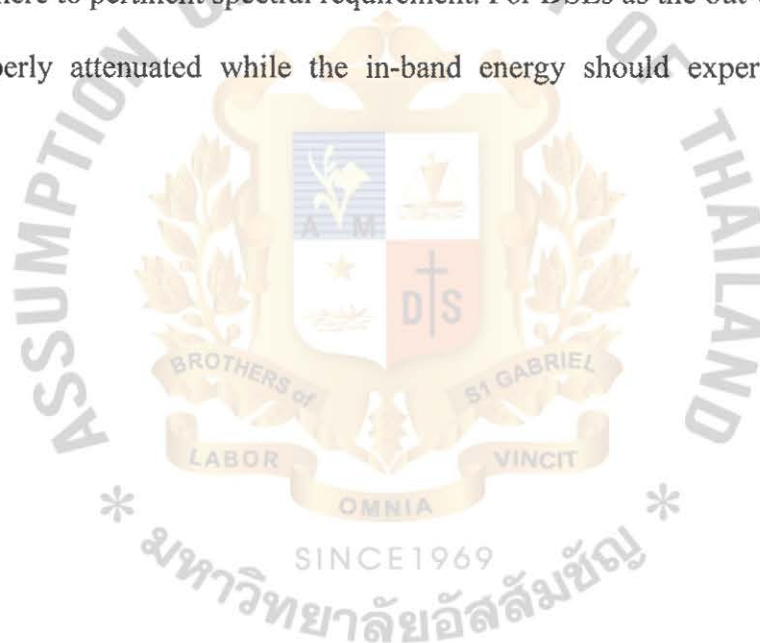
Most modern communications systems that operate near theoretical limits employ equalization in the transmitter, receiver, or both to optimize or nearly optimize transmission. Often the equalization is done digitally by adaptive digital filters. This approach provides a very flexible way to accommodate different types of channels and different types of noise environments. In most DSLs (as well as in voice-band modems), the adaptive filters converge to optimal initial settings during a training period and then can be updated during normal runtime operation of the system.

Any time a channel's frequency response is not flat over the range of frequencies being transmitted, intersymbol interference (ISI) can occur. A channel with a frequency response that is not flat is sometimes called a nonflat channel, a dispersive channel, a channel with memory, or simply a channel with ISI. Additionally, a nonflat channel has an impulse response that is nonzero at more than one point. Note that the pulse is spread out and distorted at the output of the channel. Such spreading would interfere with the next pulse transmitted. Also, a previously transmitted pulse would interfere with the one shown. A channel can have even more memory than the one shown, causing pulses or symbols to be spread out and interfere not only with immediately adjacent symbols but also with several or many of them. Equalization is mainly intended to remove some or

all of this ISI so that optimal decisions can be made on incoming symbols in the receiver.

2.15 Shaping

Shaping filters are often used at the output of a modulator. Analog or digital filters or both are used. Most often, shaping is used to ensure that the output waveforms of the transmitter adhere to pertinent spectral requirement. For DSLs as the out-of-band energy must be properly attenuated while the in-band energy should experience minimal distortion.



CHAPTER 3. LOOP ANALYSIS

3.1 ABCD Parameters

ABCD parameters are useful in characterizing two-port network. A two-port is generically defined to have a single input port and single output port with the transfer function between the two as figure 3.1.

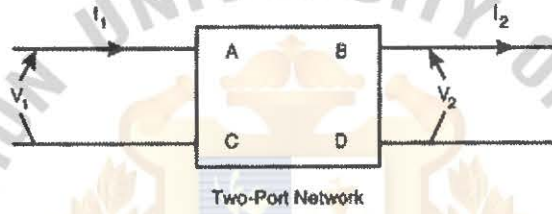


Figure 3.1 A generic two port network.

In figure 3.1, the output voltage V_2 and current I_2 are related to the input voltage V_1 and current I_1 in term of ABCD parameters as follows, [24],

$$V_1 = AV_2 + BI_2 \quad (3.1.1)$$

$$I_1 = CV_2 + DI_2 \quad (3.1.2)$$

The voltage at a point on the line is the sum of the forward traveling wave at that point and the backward traveling wave. The figure 3.2 shows a twisted pair with the forward and backward traveling waves labeled at the end of the pair ($x=L$).

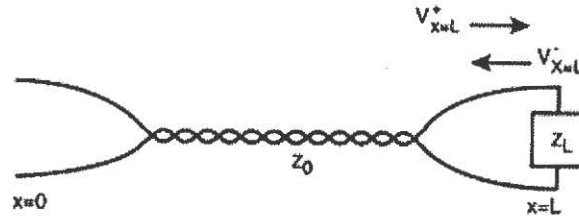


Figure 3.2 A twisted pair transmission line; the forward ($V_{x=L}^+$) and backward ($V_{x=L}^-$).

The voltage at the other end of the twisted pair ($x=0$) is

$$V(f,0) = V_{x=L}^+(e^{\gamma(f)L} + \Gamma_L(f)e^{-\gamma(f)L}) \quad (3.1.3)$$

$$\Gamma_L(f) = \frac{Z_L(f) - Z_0(f)}{Z_L(f) + Z_0(f)} \quad (3.1.4)$$

where $V(f,0)$ is the voltage at point $x = 0$, $V_{x=L}^+$ is positive traveling wave voltage, Z_0 is characteristic impedance of the twisted pair, Z_L is load impedance and Γ_L is the reflection coefficient. An equivalent two-port network for a uniform twisted pair can represent in figure 3.3.

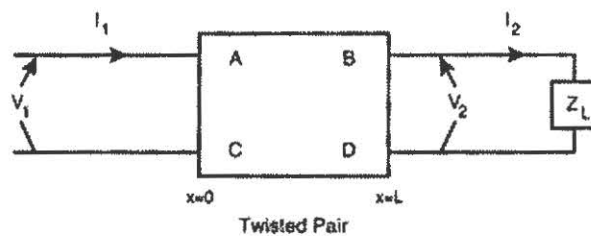


Figure 3.3 An equivalent two-port network for a twisted pair.

The expression of V_2 is given by

$$V_2 = V_{x=L}^+ + V_{x=L}^- = V_{x=L}^+(1 + \Gamma_L) \quad (3.1.5)$$

Then,

$$V_{x=L}^+ = \frac{V_2}{1 + \Gamma_L} \quad (3.1.6)$$

Substituting equation (3.1.6) into equation (3.1.3), using equation (3.1.4) and $I_2 = \frac{V_2}{Z_L}$,

then we get

$$\begin{aligned} V_1 &= \left(\frac{e^{\gamma(f)L} + e^{-\gamma(f)L}}{2} \right) V_2 + Z_0 \left(\frac{e^{\gamma(f)L} - e^{-\gamma(f)L}}{2} \right) I_2 \\ &= (\cosh(\gamma(f)L)) V_2 + Z_0 (\sinh(\gamma(f)L)) I_2 \end{aligned} \quad (3.1.7)$$

Substituting equation (3.1.7) by $I_1 = \frac{V_1}{Z_L + Z_0}$, the second two ABCD parameters that are C and D can be obtained as

$$\begin{aligned} I_1 &= \frac{1}{Z_0} \left(\frac{e^{\gamma(f)L} - e^{-\gamma(f)L}}{2} \right) V_2 + \left(\frac{e^{\gamma(f)L} + e^{-\gamma(f)L}}{2} \right) I_2 \\ &= \left(\frac{\sinh(\gamma(f)L)}{Z_0} \right) V_2 + (\cosh(\gamma(f)L)) I_2 \end{aligned} \quad (3.1.8)$$

Thus, the ABCD parameters for a uniform twisted pair are shown as

$$\begin{bmatrix} A & B \\ C & D \end{bmatrix} = \begin{bmatrix} \cosh(\gamma(f)L) & Z_0 \sinh(\gamma(f)L) \\ \frac{\sinh(\gamma(f)L)}{Z_0} & \cosh(\gamma(f)L) \end{bmatrix} \quad (3.1.9)$$

3.2 Bridge Taps

Sometimes, a twisted pair running to a subscriber might have unused twisted pair section connected at some point along its length. The other end of the unused section is left open-circuit. The unused section of twisted pair is called bridge tap. The purpose of a bridge tap is usually to leave flexibility in the location of a subscriber use in the loop. This flexibility is necessary when twisted pairs are installed prior to being used because in many cases the actual location of the subscriber is not yet known (for example, when cables are laid in a neighborhood under development). A bridge tap causes reflections at the open circuit end producing dips in the transfer function of the loop to which it is attached. Note that the propagation constant and characteristic impedance of the bridge tap might or might not be the same as the loop to which the tap is connected. Also note that the main loop itself might have different line characteristics on each side of the bridge tap. Because of bridge tap is one kind of a lumped impedance as shown in figure

3.4

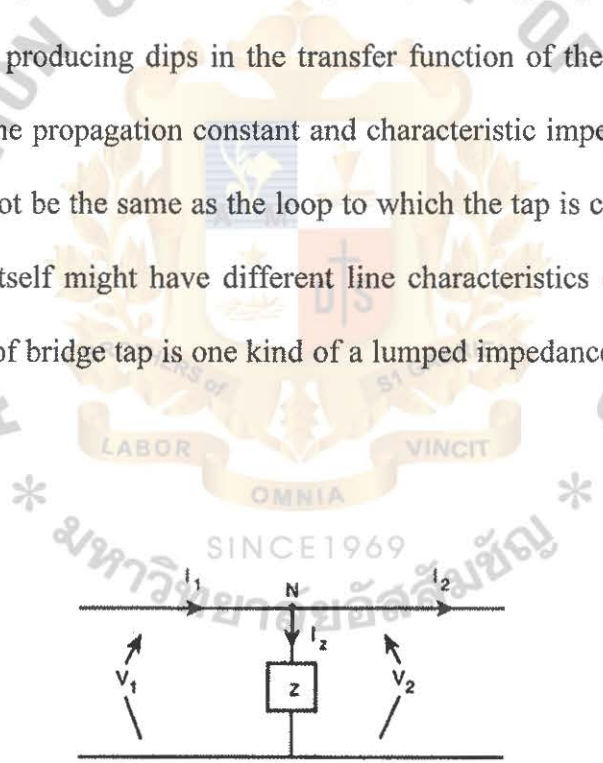


Figure 3.4 A two-port network consisting of a lumped parallel impedance

In figure 3.4, $V_2 = V_1$, then the ABCD parameter in equations (3.1.1) and (3.1.2) can be written as

$$V_1 = AV_1 + BI_2 \tag{3.2.1}$$

$$I_1 = CV_1 + DI_2 \quad (3.2.2)$$

Using Kirkoff's current law at point N, we get

$$I_1 = I_Z + I_2 = \frac{V_1}{Z} + I_2 \quad (3.2.3)$$

From equation (3.2.1) and compare equation (3.2.2) with equation (3.2.3) so it should be clear that $A = 1$, $B = 0$, $C = 1/Z$ and $D = 1$. So the ABCD matrix for a two-port network consisting only a shunt impedance is

$$ABCD = \begin{bmatrix} 1 & 0 \\ \frac{1}{Z} & 1 \end{bmatrix} \quad (3.2.4)$$

The ABCD parameters of a bridge tap are the same as any other uniform twisted pair as in equation (3.1.9). The transfer function of the tap, however does not need to be concerned because the signal does not propagate along the bridged tap.

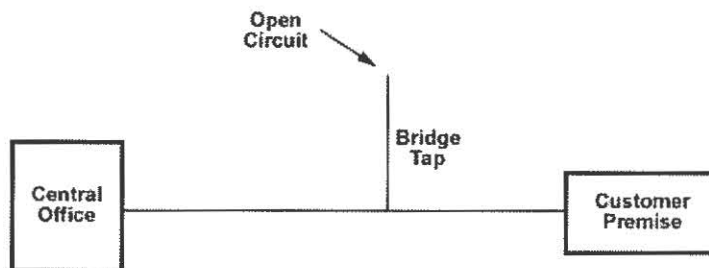


Figure 3.5 A common bridged tap configuration on a twisted pair

From figure 3.5 bridge tap is open-circuit at one end, and thus, $I_2 = 0$. Using equation (3.1.9), bridge tap's ABCD equations are

$$V_1 = \cosh(\gamma(f)L_{tap})V_2 + Z_{o,tap} \sinh(\gamma(f)L_{tap})I_2 = \cosh(\gamma(f)L_{tap})V_2 \quad (3.2.5)$$

$$I_1 = \frac{\sinh(\gamma(f)L_{tap})}{Z_{o,tap}}V_2 + \cosh(\gamma(f)L_{tap})I_2 = \frac{\sinh(\gamma(f)L_{tap})}{Z_{o,tap}}V_2 \quad (3.2.6)$$

where $Z_{o,tap}$ is the characteristic impedance of the bridge tap wire. Dividing equation (3.2.5) by equation (3.2.6), we get

$$Zin_{tap} = \frac{V_1}{I_1} = Z_{o,tap} \coth(\gamma(f)L_{tap}) \quad (3.2.7)$$

From the main loop's point of view, the effect of the bridge tap would be the same effect of a lumped impedance across the loop with the value of Zin_{tap} . The ABCD parameters of a lumped impedance were derived in equation (3.2.4). Substituting equation (3.2.7) into equation (3.2.4), the ABCD parameter will be

$$\begin{bmatrix} A & B \\ C & D \end{bmatrix}_{tap} = \begin{bmatrix} 1 & 0 \\ \frac{1}{Zin_{tap}} & 1 \end{bmatrix} = \begin{bmatrix} 1 & 0 \\ \frac{1}{Z_{o,tap} \coth(\gamma(f)L_{tap})} & 1 \end{bmatrix} \quad (3.2.8)$$

The ABCD parameters for the entire cable are found by multiplying the ABCD parameters for the individual sections along the loop. The generically one is [19]

$$ABCD_{total} = [ABCD_1][ABCD_2]... \quad (3.2.9)$$

Three important characteristics about a loop, mainly the input impedance, transfer function, and insertion loss, can be found by using ABCD parameters. For analysis of a loop, specific information beyond the ABCD parameters of the loop is necessary. This information includes the impedance of the source providing a signal to the loop, called source impedance (Z_G), and the impedance of the loop termination, called termination impedance (Z_L). Figure 3.6 shows the generic end-to-end loop model.

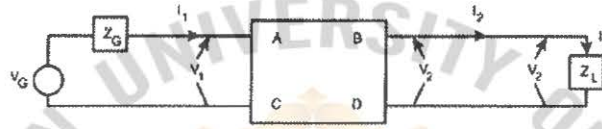


Figure 3.6 A generic end-to-end model of the loop including generator and load impedance.

Regarding to figure 3.6, by Ohm's law, it follows that $V_2 = I_2 Z_L$. Thus, the input impedance can be found as

$$Z_{in} = \frac{V_1}{I_1} = \frac{AV_2 + BI_2}{CI_2 + DI_2} = \frac{AI_2 Z_L + BI_2}{CI_2 Z_L + DI_2}$$

$$Z_{in} = \frac{AZ_L + B}{CZ_L + D} \quad (3.2.10)$$

Using $I_2 = \frac{V_2}{Z_L}$, the equation (3.1.1) can be written as

$$V_1 = AV_2 + BI_2 = AV_2 + B \frac{V_2}{Z_L} \quad (3.2.11)$$

Thus, the transfer function can be written as

$$H(f) = \frac{V_2}{V_1} = \frac{Z_L}{AZ_L + B} \quad (3.2.12)$$

The insertion loss of the loop is the ratio of power delivered to the load to the power that would have been delivered to the load without the loop presence. Essentially, this is the loss caused by inserting the loop between source and termination. If there is no loop presence, the voltage across the load could be found by

$$V_L = V_G \frac{Z_L}{Z_G + Z_L} \quad (3.2.13)$$

The power delivered to the load in this case would be

$$P_{nolop} = \frac{V_L^2}{Z_L} = \frac{V_G^2 Z_L^2}{Z_L (Z_G + Z_L)^2} \quad (3.2.14)$$

When the loop is present, the voltage V_1 can be written as

$$V_1 = V_G - I_1 Z_G \quad (3.2.15)$$

Substituting equation (3.1.2) into equation (3.2.15), comparing to equation (3.1.1) and

using $I_2 = \frac{V_2}{Z_L}$, V_2 will be

$$V_2 = \frac{V_G Z_L}{AZ_L + B + Z_G(CZ_L + D)} \quad (3.2.16)$$

The power delivered to the load with the loop presence can be found as

$$P_{withloop} = \frac{V_2^2}{Z_L} = \frac{(V_G Z_L)^2}{Z_L (AZ_L + B + Z_G(CZ_L + D))^2} \quad (3.2.17)$$

The insertion loss of the loop is given by

$$IL = 10 \log \left(\frac{P_{NoLoop}}{P_{WithLoop}} \right) = 20 \log \left(\frac{AZ_L + B + Z_G(CZ_L + D)}{(Z_G + Z_L)} \right) \quad (3.2.18)$$

3.3 Power Spectral Density

The power spectral density (PSD) of a line code defines the distribution of the line code's power in the frequency domain. A PSD mask is a template that specifies the maximum PSD allowable for a line code. PSD masks are used as both guidelines for the design and implementation of a DSL technology as well as for crosstalk modeling to simulate the benchmark performance. For DMT ADSL downstream, a common method of producing an ADSL downstream signal is describe in the figure 3.7.



Figure 3.7 Common method of producing an ADSL downstream signal

The continuous time function $v(t)$, describing the train of impulses (δ) can be written as [19]

$$v(t) = \sum_{k=-\infty}^{\infty} v_k \delta(t - kT) \quad (3.3.1)$$

where v_k is the random variable and T is the period of the line code quates. The autocorrelation function of train of impulse or R_{vv} , is

$$R_{vv}(\tau) = V^2 \delta(\tau) \quad (3.3.2)$$

where V is the height of each impulse. The normal PSD from [19] is

$$PSD = \frac{2\mathfrak{F}[R_{xx}(\tau)]}{ZT} \quad (3.3.3)$$

where Z is the reference impedance across which the signal is measured and T is the length of the baseband symbol, and $\mathfrak{F} [.]$ is Fourier transform.

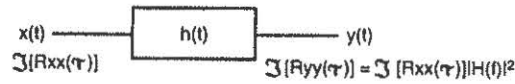


Figure 3.8 The effect of passing a signal through a linear,
time-invariant filter on the signal's PSD

Considering the figure 3.8, if the signal x with autocorrelation function R_{xx} is pass through a linear, time-invariant filter with impulse response h , the Fourier transform of the autocorrelation at the output of the filter will provide the results given by

$$\mathfrak{F}[R_{yy}(\tau)] = \mathfrak{F}[R_{xx}(\tau)] \cdot |H(f)|^2 \quad (3.3.4)$$

The PSD at the output of the ATU-C transmitter is simply the Fourier transform of autocorrelation function at the input multiplied by the squared magnitude spectrums of each of the filters between the v and the output. Given that the filter is the pulse filter, the high-pass filter (HPF), and the low-pass filter (LPF), the PSD of a downstream ADSL signal is given by [19]

$$PSD_{ADSLDS}(f) = \frac{2\mathfrak{F}[R_{vv}(\tau)] \cdot |P(f)|^2 |HPF(f)|^2 |LPF(f)|^2}{ZT}$$

where $P(f) = \frac{\sin(\pi f T)}{\pi f}$ and $P(f)$ is the pulse filter. A reasonable LPF used to filter the

ADSL downstream PSD is a fourth-order butterworth filter with a cutoff frequency of 1.104 MHz. The HPF would serve the purpose of limiting the low end of the ADSL spectrum to separate ADSL from normal Plain Old Telephone Services (POTS) traffic.

For ADSL, the reference impedance (Z) is assumed to be 100 ohms, and T is $1/(2.208 \text{ MHz})$.

$$PSD_{ADSLDS}(f) = \frac{2V^2}{ZT} \left(\frac{\sin(\pi f T)}{\pi f} \right)^2 \left(\frac{1}{1 + \left(\frac{f}{1.104 \times 10^6} \right)^8} \right) \left(\frac{f^8}{f^8 + (20 \times 10^3)^8} \right) \quad (3.3.5)$$

The PSD calculated in this model appears in figure 3.9.

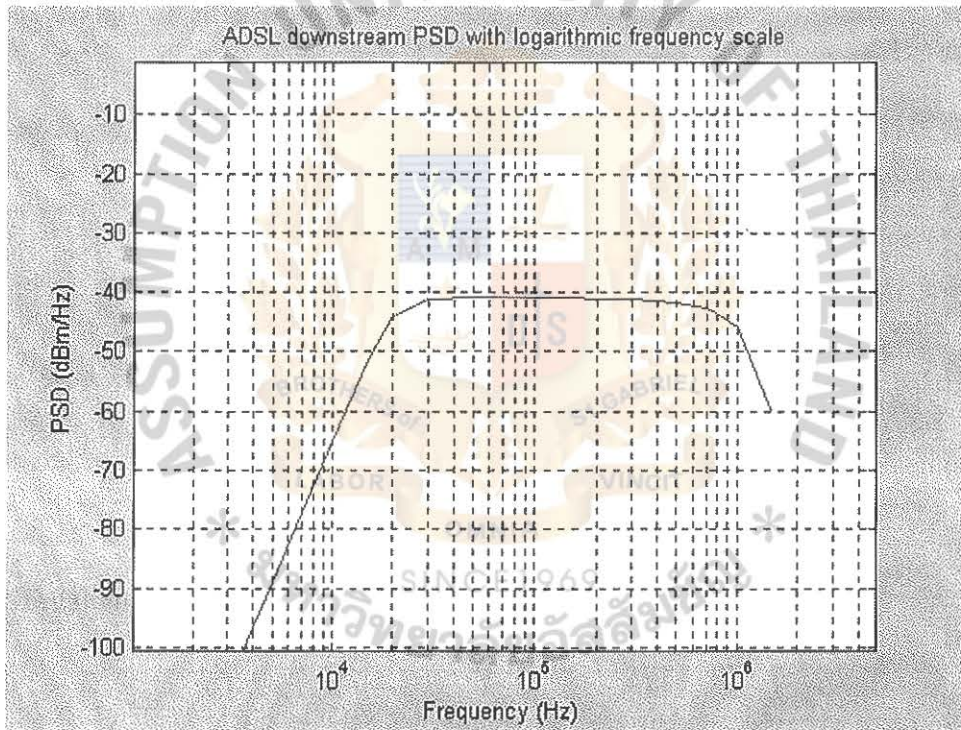


Figure 3.9 DMT ADSL downstream PSD.

Normally, the ADSL upstream signal occupies a frequency range from 25 kHz to 138 kHz. For an echo-cancelled system, the upstream PSD overlaps the downstream PSD in this region. An upstream DMT symbol can be created by passing an impulse train through a pulse filter at the rate 276,000 samples/s. The output of the pulse filter is then

send through a shaping filter. A method of producing an ADSL upstream signal is described in figure 3.10.

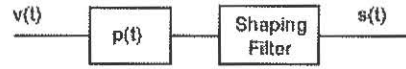


Figure 3.10 Common method of producing an ADSL upstream signal

In the original ADSL upstream PSD specification, a generic mask was used as the upstream shaping filter magnitude. Mathematically, this mask is given by [19]

$$|H_{US}(f)|^2 = \begin{cases} 10^{\frac{-38-30}{100}} & f < 138\text{kHz} \\ 10^{\frac{-38-24\left(\frac{f-138000}{4312.5}\right)-30}{100}} & f > 138\text{kHz} \end{cases} \quad (3.3.6)$$

Following the treatment of a signal pass through a filter, the output PSD can be written as

$$\begin{aligned} PSD_{ADSLUS}(f) &= \frac{2\mathfrak{I}[R_w(\tau)] \cdot |P(f)|^2 |H_{US}(f)|^2}{ZT} \\ &= \frac{2V^2}{ZT} \left(\frac{\sin(\pi fT)}{\pi f} \right)^2 |H_{US(f)}|^2 \end{aligned} \quad (3.3.7)$$

Z is assumed to be 100 ohms, and T is 1/(276000) s. An ADSL upstream PSDs can be shown in figure 3.11.

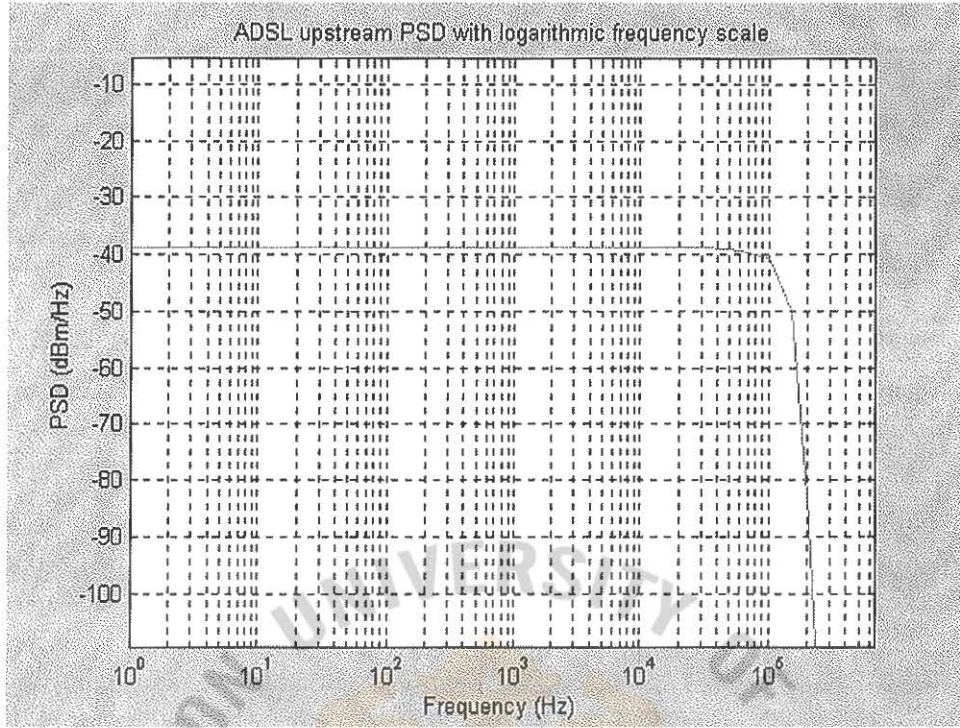


Figure 3.11 DMT ADSL upstream PSD.

3.4 Disturbers

3.4.1 NEXT disturbers

The general expression for a NEXT disturber based in the PSD of disturbing system is given by [5]

$$PSD_{NEXT}(f) = PSD_{DIST}(f) \cdot 0.882 \times 10^{-14} \cdot N^{0.6} \cdot f^{3/2} \quad (3.4.1.1)$$

where N is the number of disturbers having a PSD given by PSD_{DIST} . Note that as the number of disturbers increases, the effect of each additional disturber decreases. Graph

of the NEXT PSD for 10 ADSL downstream is shown in the figure 3.12. In addition, the normally assumed additive white Gaussian noise (AWGN) floor for a DSL line of -140 dBm/Hz is shown.

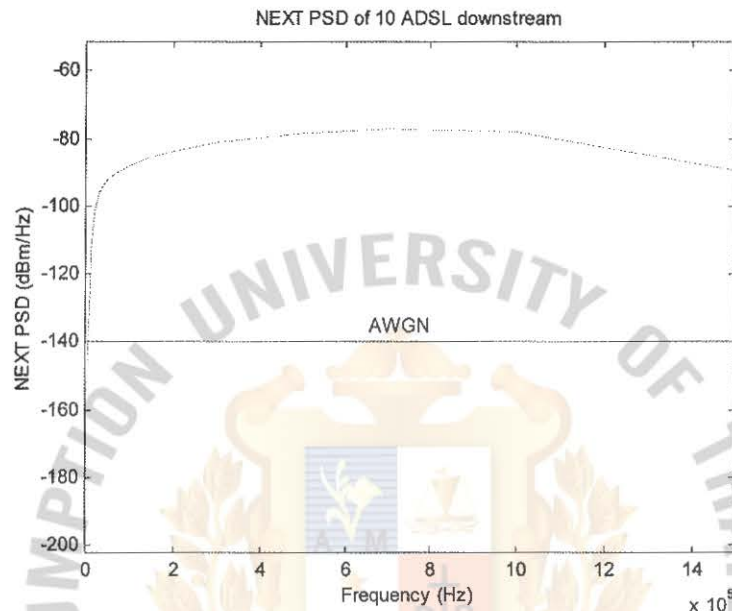


Figure 3.12 NEXT PSD of 10 ADSL downstream

3.4.2 FEXT Disturbers

The general expression for a FEXT disturber based on the PSD of the disturbing signal is given by [5]

$$PSD_{FEXT}(f) = PSD_{DIST}(f) \cdot |H_{channel}(f)|^2 \cdot K_{FEXT} \cdot L \cdot f^2 \quad (3.4.2.1)$$

Here $H_{CHANNEL}(f)$ is the channel transfer function, K_{FEXT} is a coupling constant, and L is the coupling path length. Assuming a 24 AWG with 12,000 ft. is used. Graph of FEXT for 10 downstream ADSL disturbers is shown in figure 3.13.

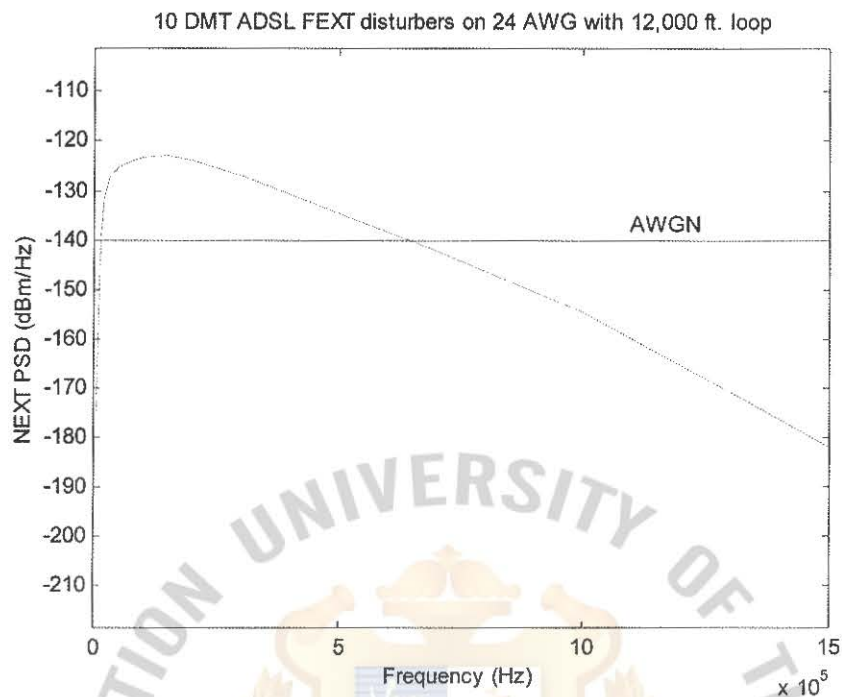


Figure 3.13 10 DMT ADSL FEXT disturbers on 24 AWG with 12,000 ft. loop.

3.5 Performance Analysis

The transmission channels of DMT approach can conceptually be viewed as in figure 3.14.

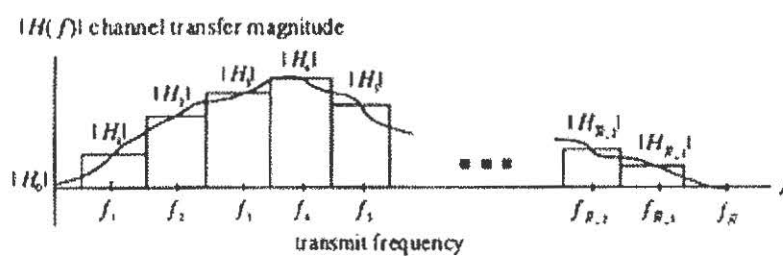


Figure 3.14 DMT decomposition of a transmission channel.

The transmission characteristic is viewed as a set of independent frequency indexed subchannels, with center frequencies, f_i , and complex channel gains H_i . Each subchannel has an SNR_i , which is useful in the performance analysis. The maximum data rate, or capacity C_i , that can be transmitted over a single flat transmission channel [21], can be computed from

$$C_i = \log_2(1 + SNR_i) \quad (3.5.1)$$

The average squared value of the complex input E_i (or the energy per complex sample) and the average square noise sample as σ_i^2 , the FFT output signal-to-noise ratio for any flat subchannel is [10]

$$SNR_i = \frac{E_i |H_i|^2}{\sigma_i^2} \quad (3.5.2)$$

A well-known result from information theory is that the capacity of a set of independent channels is the sum of the capacities of the individual subchannels. The DMT system should allocate amount of energy to each of the subchannels such that overall capacity $C = \sum_i C_i$ is maximized subject to a total energy constraint $E = \sum_i E_i$. The method that will use is called water-filling. The energy is viewed as water that can be poured into a bowl (curve), that represents essentially the inverse SNR of the transmission medium $[\sigma^2(f)/|H(f)|^2]$, until no more water (energy) is left. Clearly, the subchannels with the highest transmission gain comparing to noise get the most energy and some

subchannels may not get any energy. The optimum energy is just the amount occurring at each frequency.

3.6 The SNR Gap

The SNR gap is a useful concept that characterizes how close a given code on a subchannel is to its theoretical maximum for that particular subchannel and its given transmit energy [10]. An uncoded constellation that transmits b_i bit per successive value of E_i on subchannel i is characterized by the quantity d_i^2 , the distance between any two closest points. The energy for a square constellation is [8]

$$E_i = \frac{2^{b_i} - 1}{6} d_i^2 \quad (3.6.1)$$

This energy computation is exact when b_i is an even integer. However, it can be used for any value of b_i accurately when coding is used. Any small deviations are incorporated into a second coding parameter called the coding gain. Coding improves the distance d_i^2 over sequences of transmissions with a resultant improvement in d_i^2 with respect to uncoded transmission on the square constellation. The improvement is called the coding gain γ_c . The probability of the error of this code on a channel with gain H_i and $d_{\min,i}^2 = |H_i|^2 \cdot d_i^2 \cdot \gamma_c$ is

$$P_{e,i} \approx 4Q\left(\frac{d_{\min,i}}{2\sigma_i}\right) \quad (3.6.2)$$

Where the Q-function argument is [8]

$$Q(x) = \int_x^{\infty} \frac{1}{\sqrt{2\pi}} \exp\left(-\frac{x^2}{2}\right) dx \quad (3.6.3)$$

The SNR gap or Γ_i can be written as [8]

$$3\Gamma_i = \frac{d_{\min,i}^2}{4\sigma_i^2} \quad (3.6.4)$$

With algebraic manipulation, one determines that the number of bits that are being transmitted with this code is [7]

$$b_i = \log_2 \left(1 + \frac{SNR_i}{\Gamma_i} \right) \quad \text{or} \quad \Gamma_i = \frac{SNR_i}{2^{b_i} - 1} \quad (3.6.5)$$

For uncoded transmission and probability of error of 10^{-7} , one finds that the SNR gap is 9.8 dB [5], meaning that 9.8 dB is lost with respect to an optimally coded system and SNR_i is signal-to-noise ratio of each subchannel. The total transmission throughput, R , is the product of prefix modified baud rate and the number of bits each baud carries [5] as

$$R = \frac{1}{T} \sum_{i=1}^{256} \log_2 \left(1 + \frac{SNR_i}{9.55} \right) \quad (3.6.6)$$

Where 9.55 is SNR gap for uncoded transmission and probability of error of 10^{-7} , $1/T$ is the modified baud rate. That is, [5]

$$\frac{1}{T} = \frac{2.2 \times 10^6}{512 + 32} = 4044 \text{ Hz} \quad (3.6.7)$$

Assume that the FFT size is 512, the sampling rate is 2.2 MHz, and a guard period of 32 sampling points is used.

3.7 POTS Splitter

A POTS splitter separates the 300 Hz to 3,500 Hz voice channel from the upstream and downstream channels. In the voice passband, the POTS splitter should pass not only voice frequency signal, but also dial tone, ringing, and on/off hook signals. For the voice frequency signal, the POTS splitter should maintain original POTS impedance. The structure of a POTS splitter is similar for both ATU-C and ATU-R. A POTS splitter consists of mainly a lowpass filter for the POTS interface and a highpass filter for upstream and downstream channels. The lowpass filter removes the interference from upstream and downstream channels to the POTS channel. The POTS channels impedance, which is about 600 ohms, should not be effected by the impedance of upstream and downstream channels, which is about 100 ohms [5]. The highpass filter removes the interference from the POTS channel to upstream and downstream channels. The harmonics of ringing and on/off hook signal should especially be prevented from entering upstream and downstream channels. The figure 3.15 shows the circuit diagram of a POTS splitter.

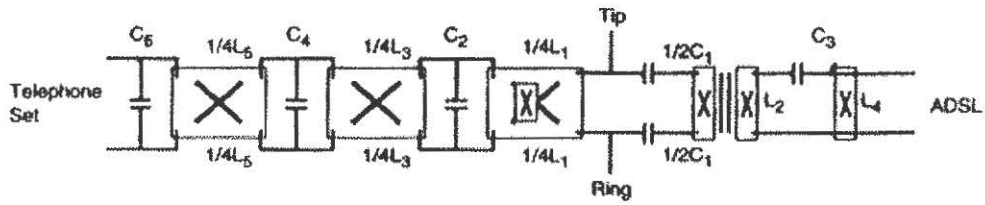


Figure 3.15 Circuit Diagram of a POTS Splitter.

The inductors for the lowpass filter should have high Q for small signal attenuation and high current saturation levels to avoid generating harmonics under the heavy drive of high intensity voltage or current. A stopband loss of 70 dB is required for both lowpass and highpass filters. Because of the narrow guard band, a slope of -60 dB per decade is also required. The figure 3.16 shows required lowpass and highpass frequency responses for a POTS splitter. [5]

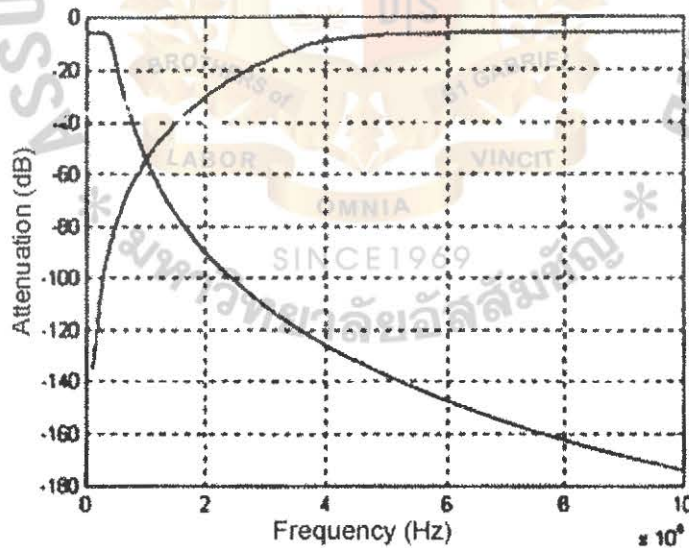


Figure 3.16 Desired Lowpass and Highpass Frequency Responses for a POTS Splitter

The highpass filter for ADSL is at the right side of the POTS input, and the lowpass filter for the telephone set is at the left side, as illustrated in figure 3.15. Only POTS and telephone interfaces need balanced design. The highpass filter is a fourth-order filter

with balanced input for the POTS fine and unbalanced output for the ADSL transceiver. The lowpass filter is a seventh-order filter with balanced input and output ports. These filters can be first designed according to the conventional unbalanced structure. The capacitance for the balanced part of the highpass filter is simply twice that calculated for the unbalanced structure. The inductance of the lowpass filter is a quarter of that calculated for the unbalanced structure, assuming a coupling coefficient of approximately one between two inductors sharing the same magnetic core. The lowpass filter part of the POTS splitter is an LC ladder. Values for L's and C's can be calculated according to the following formula: [5]

$$L_{2m-1} = \frac{2R_1 \sin\left(\frac{(4m-3)\pi}{2n}\right)}{\omega_c} \quad (3.7.1)$$

$$C_{2m} = \frac{2 \sin\left(\frac{(4m-3)\pi}{2n}\right)}{R_1 \omega_c} \quad (3.7.2)$$

For $m = 1, 2, 3$, $n = 6$, $R_1 = 600$, $\omega_c = 2\pi \times 4\text{kHz}$, we have $L_1 = 2.06 \text{ mH}$, $L_3 = 7.68 \text{ mH}$, $L_5 = 5.627 \text{ mH}$, $C_2 = 0.5627 \text{ }\mu\text{F}$, $C_4 = 0.768 \text{ }\mu\text{F}$, and $C_6 = 0.206 \text{ }\mu\text{F}$.

These L's and C's values result to Butterworth filter frequency response. A fourth-order lowpass filter can be first designed and then transformed to a highpass filter.

For $m = 1, 2$, $n = 4$, $R_1 = 100$, $\omega_c = 2\pi \times 4\text{kHz}$ we have $L'_1 = 0.3045 \text{ mH}$, $L'_3 = 0.7352 \text{ mH}$, $C'_2 = 0.07352 \text{ }\mu\text{F}$, and $C'_4 = 0.03045 \text{ }\mu\text{F}$. The corresponding highpass filter component values are as follow by using formula [5]:

$$C_i = \frac{1}{\omega_c^3 L_i'} \text{ and } L_i = \frac{1}{\omega_c^3 C_i'} \quad (3.7.3)$$

Then, $C_1 = 0.052 \text{ mF}$, $C_3 = 0.0215 \text{ mF}$, $L_2 = 0.21 \text{ mH}$, $L_4 = 0.52 \text{ mH}$.



CHAPTER 4. THE CASE STUDY OF ADSL IN THE HOTEL

The Sukhothai Hotel (Bangkok) is the first hotel in Thailand that uses ADSL system to provide the high speed internet access and video on demand services to clients. The Lucent ADSL concentrator (Stinger) has been selected to be the backbone of the system. Stinger is the new ATM-based DSL Access Concentrator that was released by Lucent in October 1999. In each room, Sukhothai Hotel has installed a Cellpipe which is the ADSL modem by Lucent. Cellpipe uses the DMT based system and provides up to 8 Mbps downstream and up to 1 Mbps upstream. The network of Sukhothai Hotel is illustrated in figure 4.1:

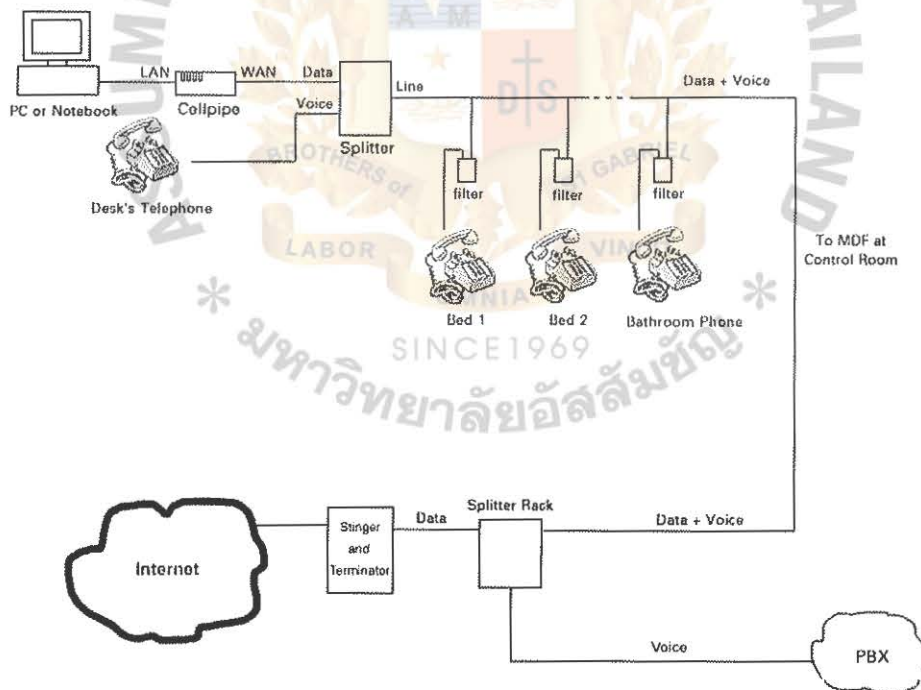


Figure 4.1 Network of Sukhothai Hotel

4.1 Low Pass Filter

The normal configuration of the ADSL access network is shown in figure 4.2. The POTS Splitter in figure 4.2 is used to separate both voice band signal and the ADSL signal as shown in figure 4.3.

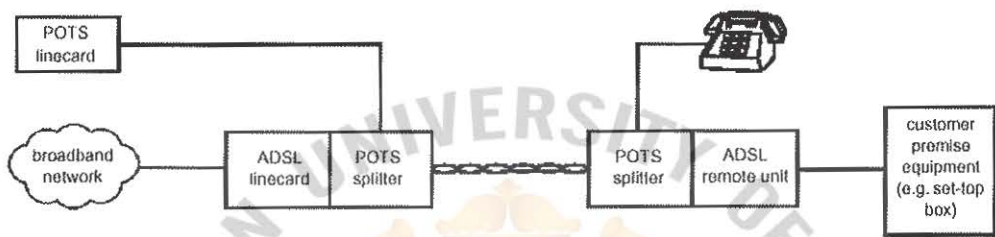


Figure 4.2 ADSL in the access network

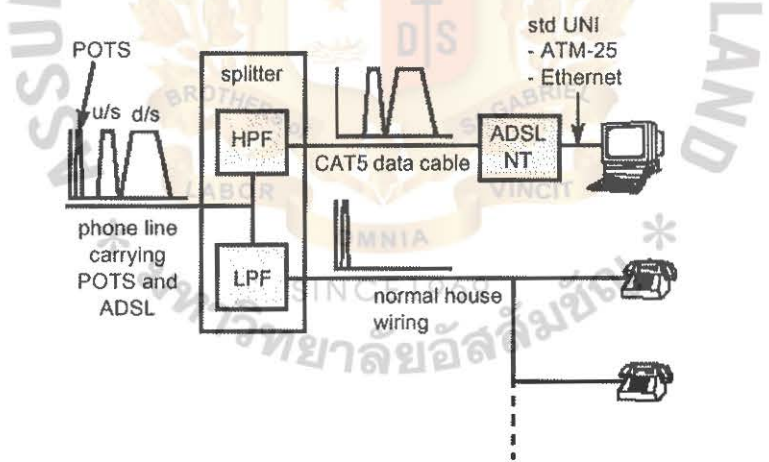


Figure 4.3 Purpose of splitter filter

The technicians of the hotel just arbitrary split the main telephone line for every point that needs to use telephone system, starting from bathroom, bed 2, bed 1, and so on until the desk as shown in the figure 4.1. This splitting behavior causes the problem. Using POTS Splitter feature from figure 4.2 to solve the problem at every point is too

expensive. The Low Pass Filter from figure 4.3 is therefore developed to be used instead. The low pass filter can separate the voice band (< 4 kHz) from ADSL upstream and downstream band (25 kHz – 1.1 MHz). The figure 4.4 shows the schematics of the Low Pass filter that limits the passband cutoff at 4 kHz and stopband cutoff at 8 kHz by using Chebyshev method. This Low Pass filter will be installed to every bridge tap (or telephone outlet) in the room for the purpose of separating the voice band. The frequency response of Low Pass Filter and characteristic impedance of the Low Pass Filter are shown in the figure 4.5 and figure 4.6 respectively.

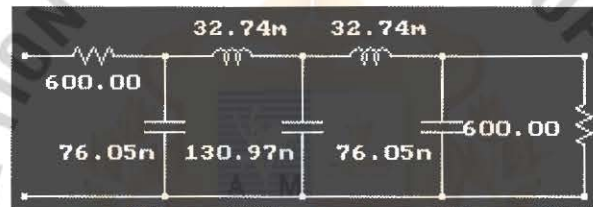


Figure 4.4 Low Pass Filter Schematic

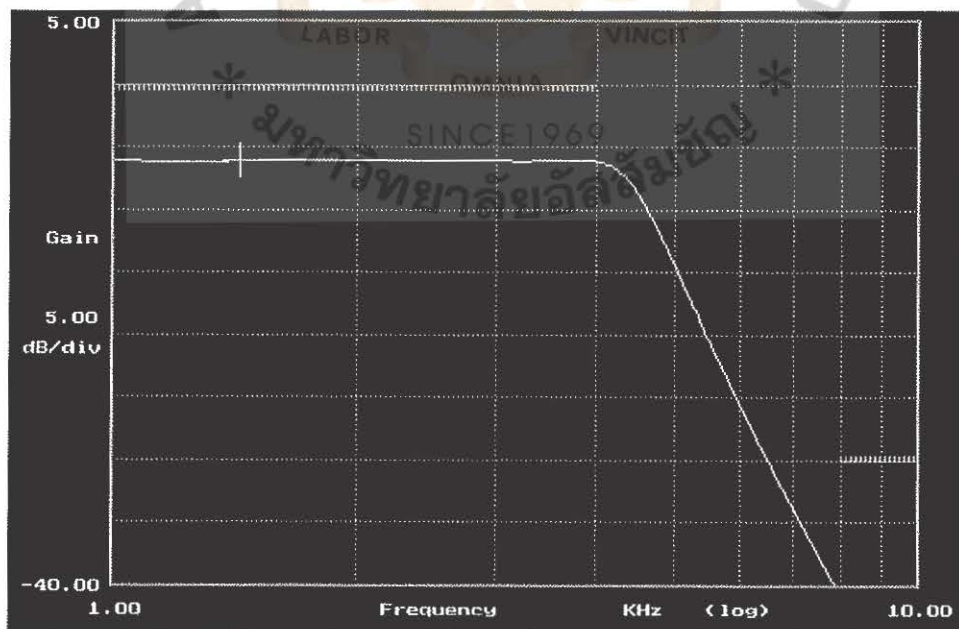


Figure 4.5 Frequency response of the Low Pass Filter

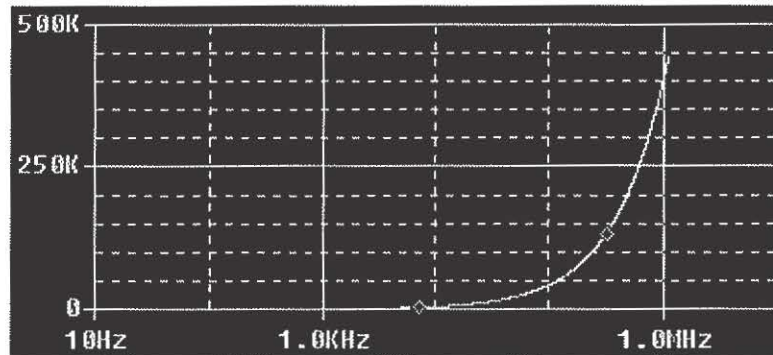


Figure 4.6 The characteristic impedance of the Low Pass Filter

4.2 Simulation and Measurement

4.2.1 Simulation

The Sukhothai hotel has many types of rooms (Superior, Deluxe, Executive Suites, Deluxe Suits, Garden Suites, and Sukhothai Suites). The superior is quite small with only 2 telephone outlets in the bathroom and at the desk (only 1 bridge tap). The largest room is Sukhothai Suites which have 11 telephone outlets (10 bridge taps). This means the lowest bridge tap for this environment is 1 and the highest bridge tap is 10. The distance between each bridge tap is about 5 metres and each bridge tap is 5 metres long. This can be shown in the figures 4.7 and 4.8.

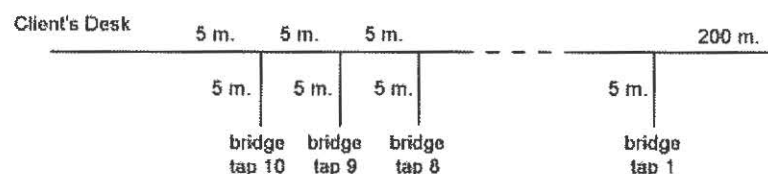


Figure 4.7 Bridge tap detail for room 253

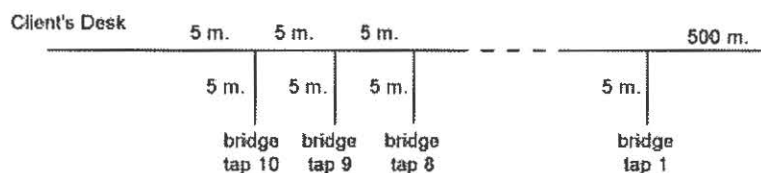


Figure 4.8 Bridge tap detail for room 556

By testing the ADSL upstream and downstream rate at the nearest room (room number 253) from the Stinger, which is about 200 metres and the farthest room (room number 556) from the Stinger is about 500 metres. Software in Appendix B. is used for simulation the transfer function, insertion loss, signal to noise ratio and data rate approximate for downstream and upstream of the line by using 24 NEXT, 24 FEXT and AWGN. The effect of impulse noise is not included in this software: it is assumed that a good forward error correction code has been selected to effectively handle impulse noise. Using the Software in Appendix B. and simulation parameter in Table 4.1. simulate the effect of transfer function, insertion loss and signal to noise ratio for these 2 rooms. It can be shown in the figures 4.9 thru 4.16, respectively.

FFT/IFFT size	256
Bandwidth of subcarrier	4.3125 kHz
Symbol Rate	4 kHz
Bandwidth	1.104 MHz
White Noise	-140 dBm/Hz
Bit Error Ratio	10E-7
Transmission Power (Downstream/Upstream)	-40/-38 dBm/Hz
Coding Gain	0 dB
Cable	24 AWG (0.4 mm.)

Table 4.1 Simulation Parameters

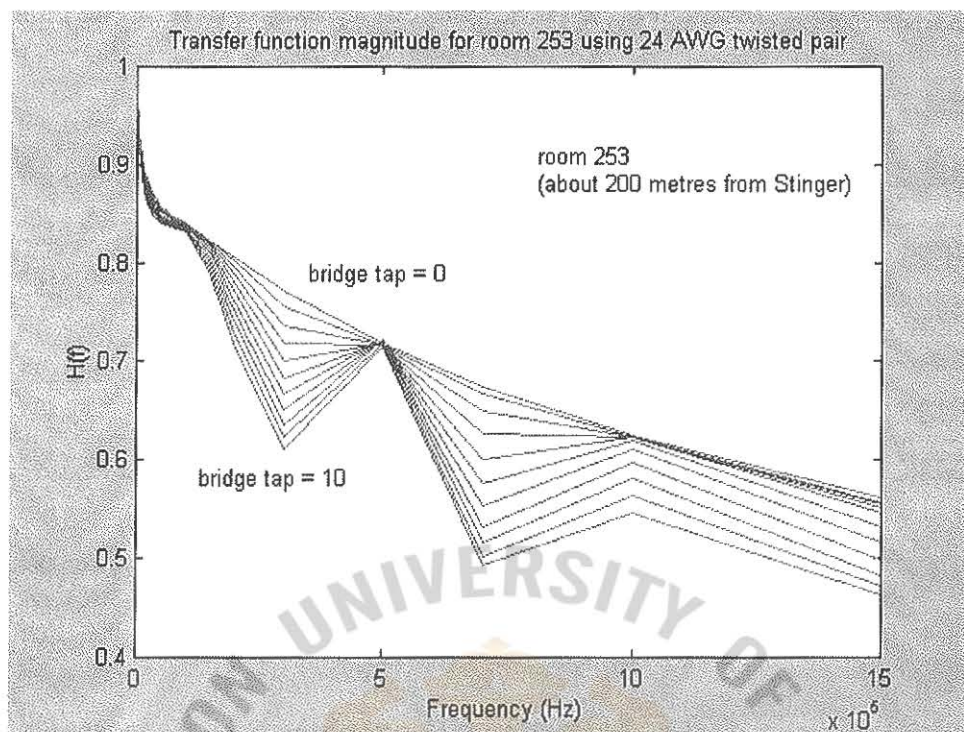


Figure 4.9 Transfer function magnitude for room 253 (about 200 metres from Stinger)

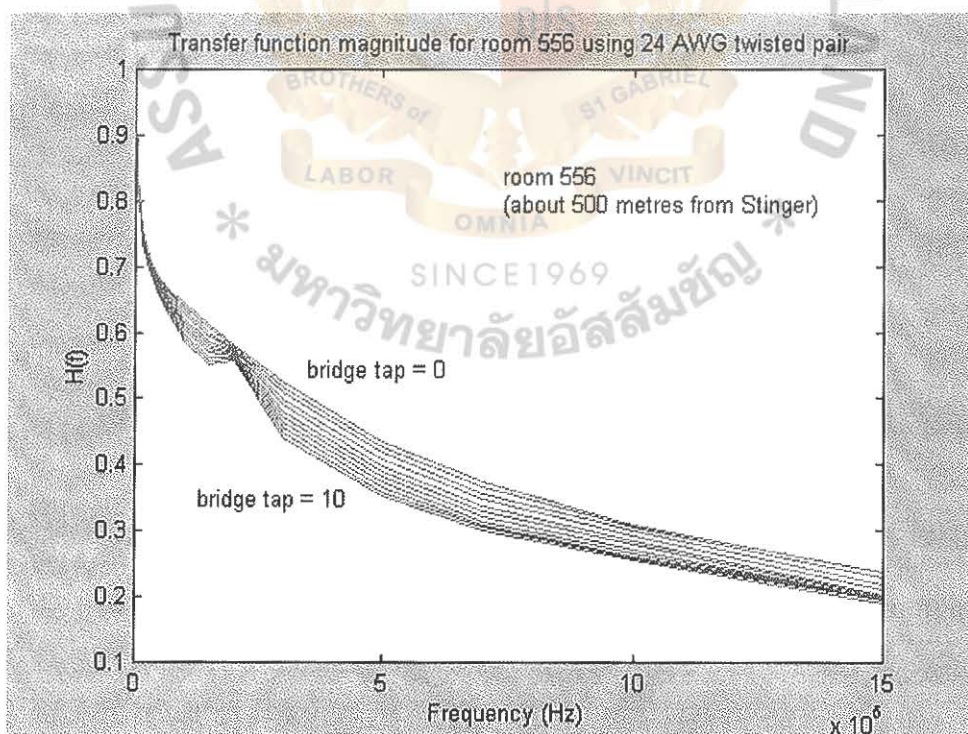


Figure 4.10 Transfer function magnitude for room 556 (about 500 metres from Stinger)

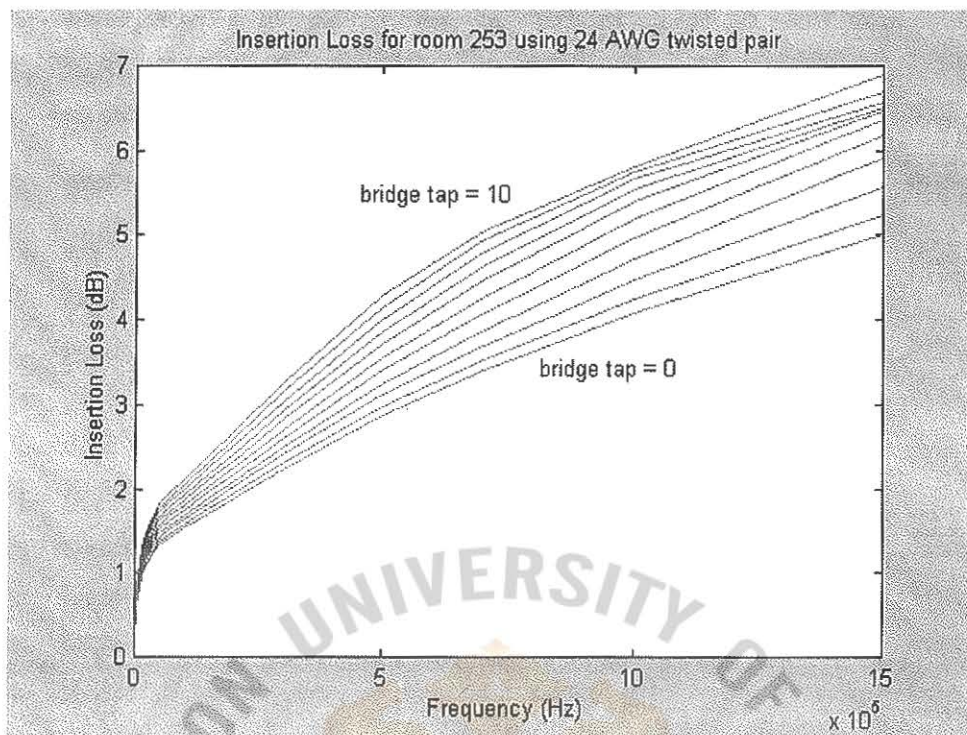


Figure 4.11 Insertion Loss for room 253 (about 200 metres from Stinger)

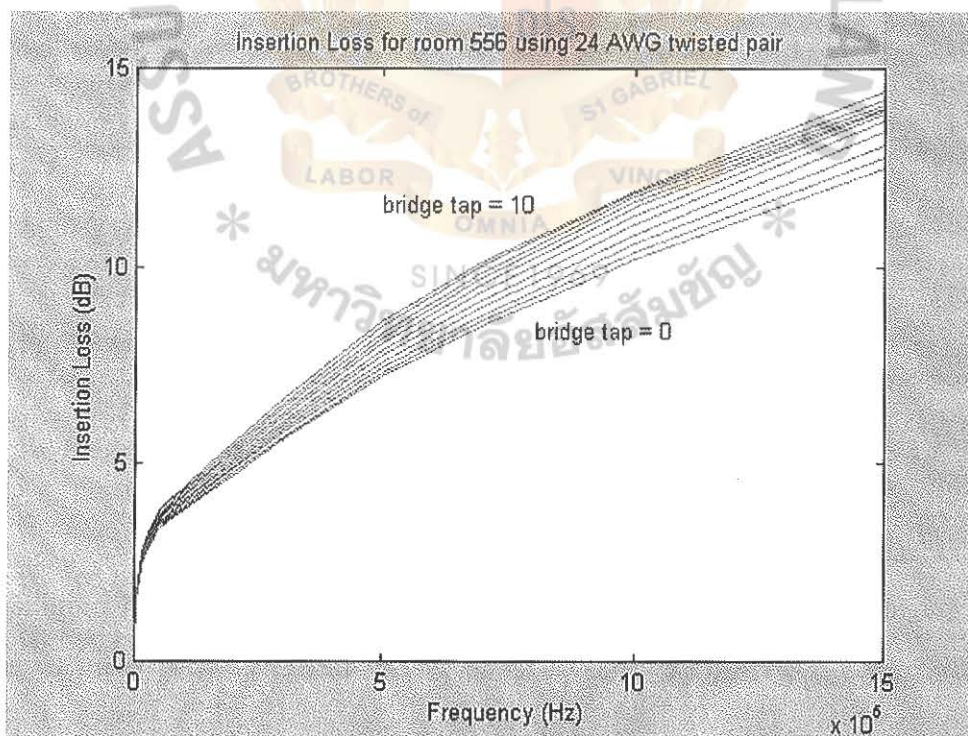


Figure 4.12 Insertion Loss for room 556 (about 500 metres from Stinger)

SNR for room 253(downstream) with 24 DMT downstream FEXT, 24 DMT upstream NEXT and AWGN

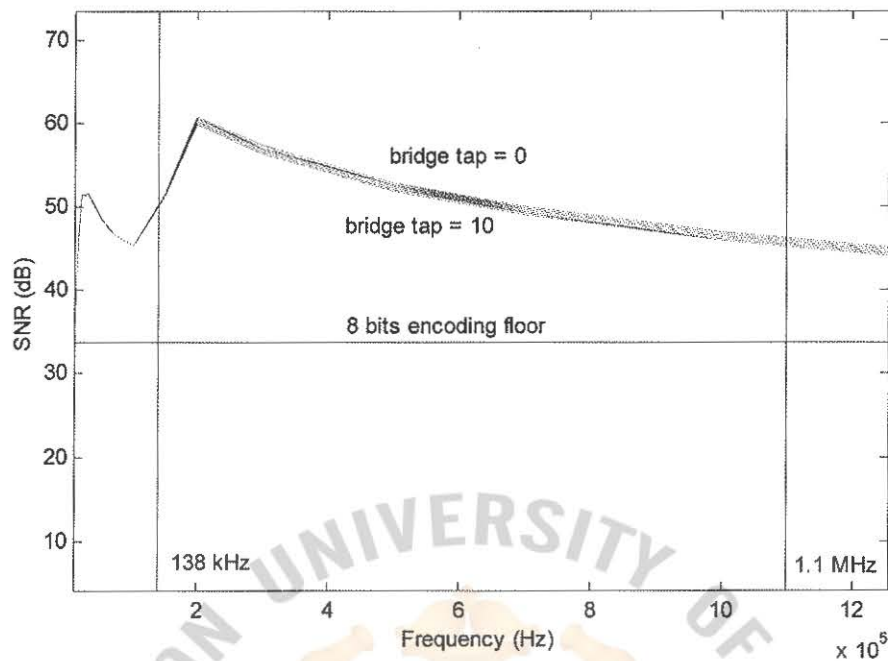


Figure 4.13 SNR for room 253(downstream) with 24 DMT Downstream FEXT, 24 DMT Upstream NEXT and AWGN

SNR for room 253(upstream) with 24 DMT upstream FEXT, 24 DMT downstream NEXT and AWGN

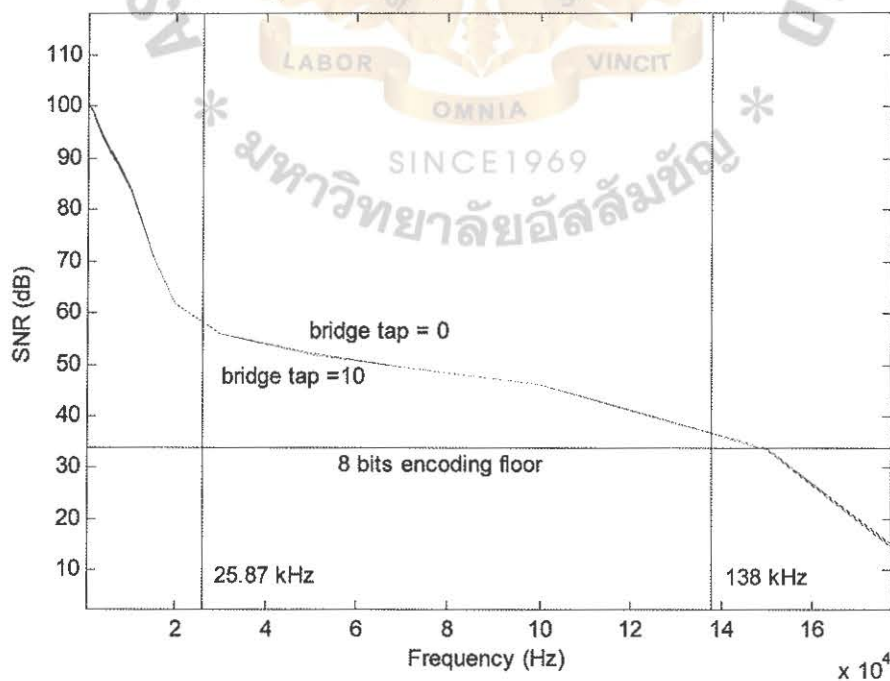


Figure 4.14 SNR for room 253(upstream) with 24 DMT Upstream FEXT, 24 DMT Downstream NEXT and AWGN

SNR for room 556(downstream) with 24 DMT downstream FEXT, 24 DMT upstream NEXT and AWGN

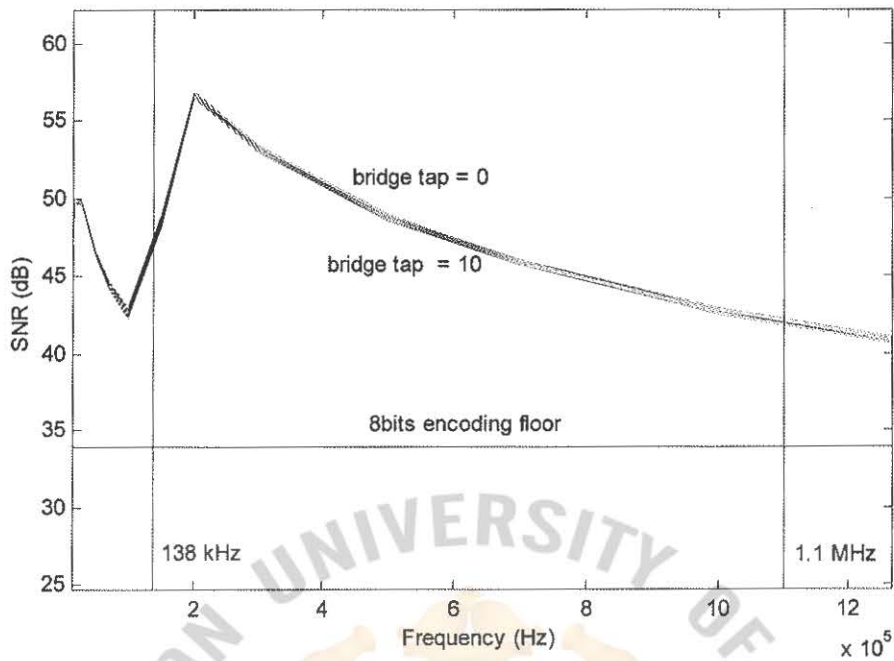


Figure 4.15 SNR for room 556(downstream) with 24 DMT Downstream FEXT, 24 DMT Upstream NEXT and AWGN

SNR for room 556(upstream) with 24 DMT upstream FEXT, 24 DMT downstream NEXT and AWGN

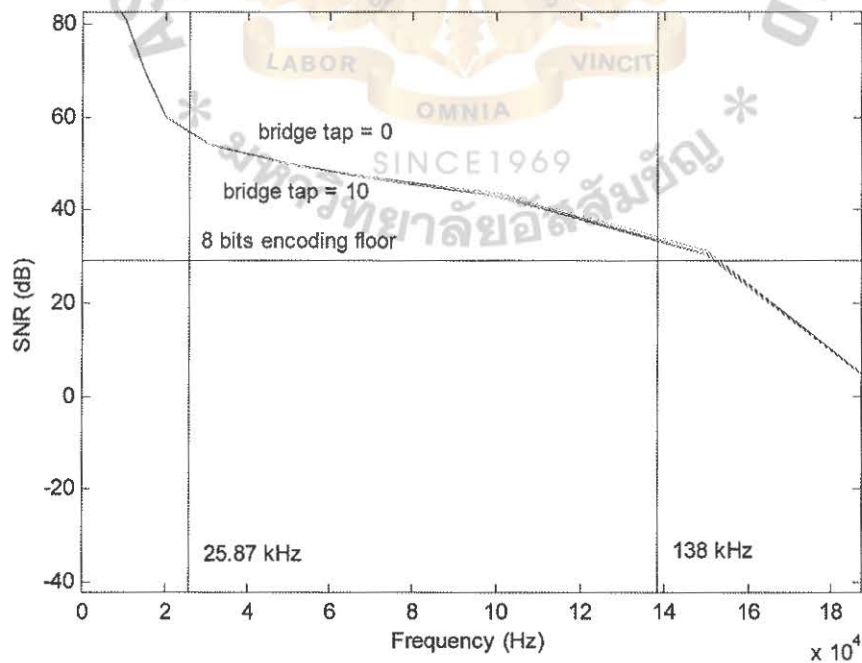


Figure 4.16 SNR for room 556(upstream) with 24 DMT Upstream FEXT, 24 DMT Downstream NEXT and AWGN

The result from figures 4.9 and 4.10 shows that the effect of the bridge taps 5 metres long to the transfer function of both rooms are not equal. It depends on the bridge taps length and the main loop length in this case the room 253 has the main loop length about 200 metres long and bridge taps 5 metres long has more severe than room 556 that has the main loop length about 500 metres with the same bridge tap length. And figure 4.11 and 4.12 shows the insertion loss of room 253 and 556 respectively.

The results from figures 4.13, 4.14, 4.15 and 4.16 show that the signal to noise ratio of both rooms is much higher than the highest encoding of 8-bits levels or maximum data transfer rate. So the data transfer rate of upstream and downstream for both rooms can go up to maximum data transfer rate. This situation can occur to both rooms because the main loop lengths of both rooms are quite short and from the simulation result it's show that the effect of bridge tap to the data transfer rate is quite small. When the loop length is increase, the signal to noise ratio is drop down more severe than the effect of bridge tap. So from Matlab simulation in figures 4.17 and 4.18, it is shown that the maximum distance that downstream data transfer rate still maximum is 2.25 km and the maximum distance that upstream data transfer rate still maximum is 1.2 km. The data rate versus loop length can be shown in figure 4.19.

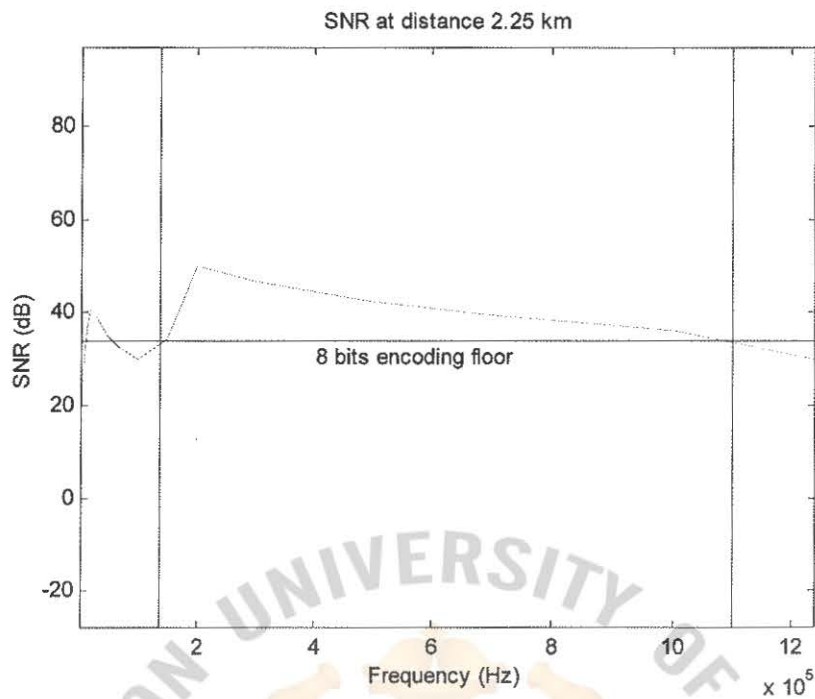


Figure 4.17 SNR at distance of 2.3 km, with 24 DMT Downstream FEXT, 24 DMT Upstream NEXT and AWGN

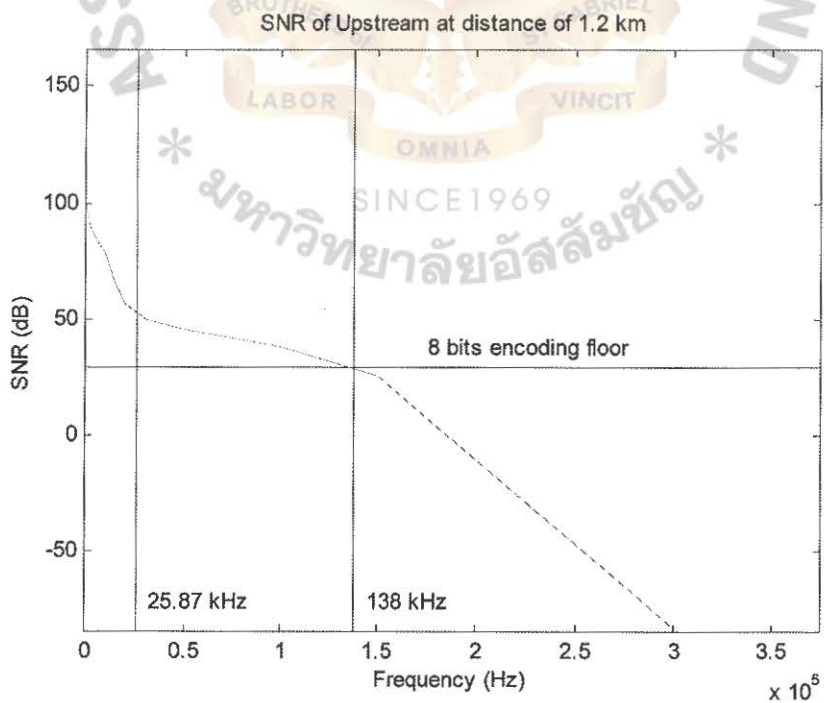


Figure 4.18 SNR at distance of 1.2 km, with 24 DMT Upstream FEXT, 24 DMT Downstream NEXT and AWGN

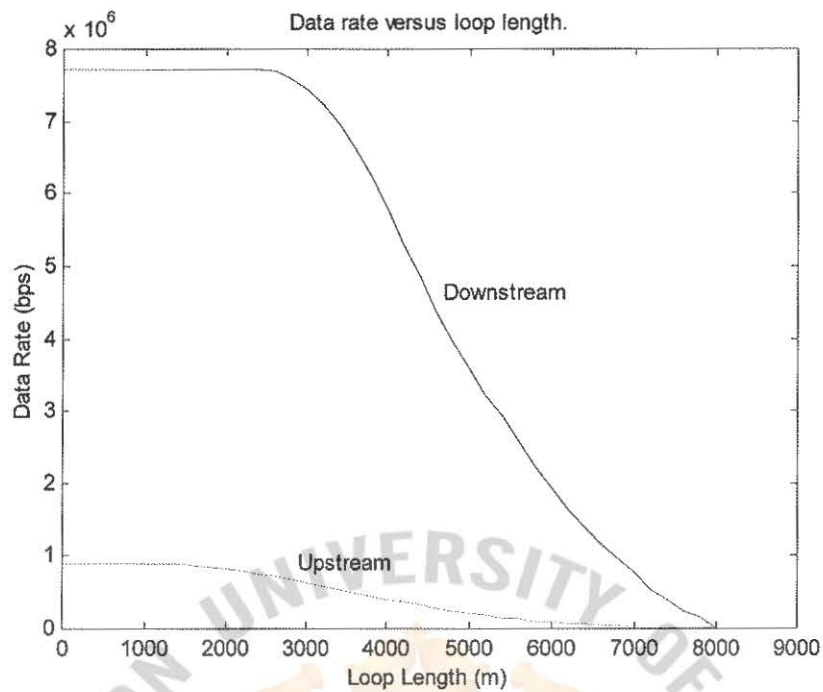


Figure 4.19 Data rate versus loop length. Impairments are 24 DMT Downstream FEXT, 24 DMT Upstream NEXT and AWGN at -140 dBm/Hz.

4.2.2 Measurement

By using Qcheck software to check the upstream and downstream bit rate at room number 253 and 556, the results are shown in figures 4.20 and 4.21.

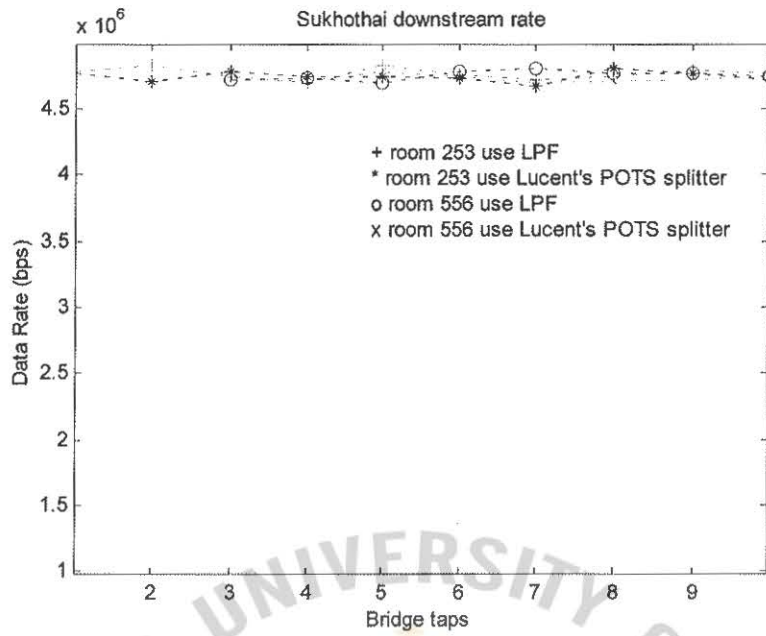


Figure 4.20 Downstream bit rate at Sukhothai Hotel

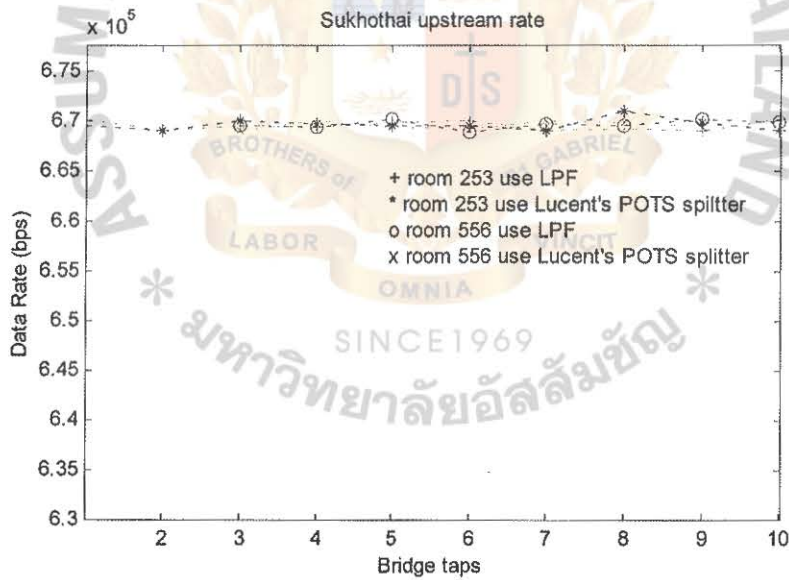


Figure 4.21 Upstream bit rate at Sukhothai Hotel

The results in figures 4.20 and 4.21 show that the effect of bridge taps to the room number 253 and room 556 is almost negligible because the signal to noise ratio of both rooms is higher than the highest encoding (8 bits/subchannel) signal to noise ratio as the simulation result in figures 4.13, 4.14, 4.15, and 4.16.

4.2.3 Comparison

Theoretically, the data rate is [13]

The data rate = (number of channels) x (number of bits/channel) x (modulation rate)

So downstream rates of both rooms are equal to $8 \times 224 \times 4000 = 7.168$ Mbps and $8 \times 26 \times 4000 = 832$ kbps for upstream (Stinger uses subchannel number 6 to 31 for upstream and subchannel number 32 to 255). The data rate shown in figures 4.20 and 4.21 is lower than the rate that we suppose to have because Stinger is ATM based system and also because the results of figures 4.20 and 4.21 were measured by software, running on IP datagram application. The IP datagram uses Ethernet frame format as shown in the figure 4.22 [22], so the header of Ethernet frame format must be included with ATM overhead [20] in figure 4.23.

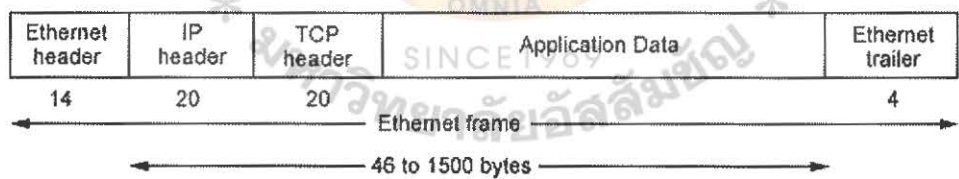


Figure 4.22 Ethernet frame format.

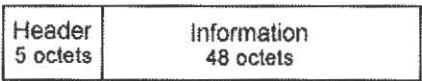


Figure 4.23 ATM transmission cell

In theory, the baud rate of 4.3125 kHz can be used to calculate the data transmission rate directly. But in practice, the baud rate cannot be greater than 3.8 kHz [4]. At this practical baud rate, the data transmission rate is much lower than the theoretical data transmission rate.

4.2.4 Recommendations

From simulation and measurement, it's shown that ADSL can apply to use with the hotel network or enterprise network very well compare to other technologies under the condition that hotel services cannot be interrupt cause of re-wiring the new network cable. Wireless is another technology that can implement under the condition above and can provide data transfer rate up to 10 Mbps. However wireless network is difficult to upgrade and support to the hotel customers so ADSL system is the best solution for the hotel network today.

4.3 Cost Analysis

The ADSL concentrator (Stinger) can have maximum 14 Line Interface Modules and 14 Line Protection Modules, if we use 24 Ports ADSL Line Interface Module for all 14 Ports available on the Stinger that means it can provide up to 336 connections or 336 rooms. Every room need to install 1 Cellpipe (ADSL Modem), 1 DSL-VSP (POTS Splitter) and 2 Low Pass Filter. At the PBX room of the Hotel need to have 336 DSL-VSP (POTS Splitter) to separate ADSL signal and Voices band and 1 DSL terminator to convert the ATM backbone network back to Ethernet. By using the price list in

Appendix C. , the total cost for installing 336 rooms to use ADSL system is 5.9 million Baht or 1 room is cost 17,563 Baht.



CHAPTER 5. CONCLUSION

Asymmetric Digital Subscriber Lines (ADSL) can supply the necessary bandwidth for applications such as fast access to the Internet, video conferencing, interactive multimedia, and Video-on-Demand. This technology is designed to solve the most severe bottleneck in the data access network between the Central Office and the customer, or end-user. ADSL is a huge step in the data communication. It combines the wide frequency spectrum (up to 1.1 MHz) of the existing copper wire with an advanced coding/decoding method. So ADSL is considered as one of the high bit rate data transmission technologies.

In the small system, like the hotel environment, it has more bridge taps than the normal ADSL system. For the internal telephone system purpose, using POTS Splitter to separate the voice band for every bridge tap in the hotel is too expensive. As a result of this thesis, the low cost Low Pass Filter is developed to be used instead of the POTS Splitter. It can be used effectively to separate the voice band. The result of measurement has shown that the data transmission rate obtained by using the designed Low Pass Filter is almost the same as using POTS Splitter. Therefore, this Low Pass Filter is recommended to be a good solution for the hotel environment.

The Matlab Software uses DMT signaling scheme to simulate the effect of the number of bridge taps and the loop length on the transmission bit rate capability. The impairments considered are DMT downstream FEXT, AWGN and NEXT from DMT upstream. The software use the information of the transfer functions, insertion loss, signal to noise ratio to approximate the transmission bit rate of that loop plant. The

simulation result has shown that the software can accurately estimate the transmission bit rate compare to measurement result from the hotel. From the simulation and measurement, it is shown that ADSL backbone system can be used over the existing telephone loop of the hotel environment. The effect of impulse noise and AM radio interference in hotel environment are not included in this thesis.

In the future, ADSL for the enterprise system, like the hotel network, will become more popular in Thailand because it can overcome the wiring limitation and has the lower cost than installing the complete ethernet based local area network. By the end of this year, there will be many hotels in Thailand that will use ADSL as the hotel's backbone system. Consequently, this thesis is going to be very useful, as it can provide many critical ideas about ADSL transmission characteristic.

Future Work

Nowadays, the ADSL system has become more and more popular in Thailand, although the ADSL equipments have to be imported from foreign countries at the high cost. Among all ADSL equipments, ADSL modem is one of the most important equipments. If we can develop and produce the ADSL modem in Thailand, we will be able to purchase the ADSL modem at much cheaper price. This will certainly help decrease much of the cost of system development. Thai people have sufficient knowledge and competence to develop and produce the ADSL modem. Therefore, the recommendation is that we should try to develop and invent the ADSL modem in order to reduce the system development cost and to enhance the competence of Thai engineers.

APPENDIX A.

A.1 22 and 24 AWG Characteristic

Table A.1 22 AWG Characteristic at 70 Degrees F

Frequency (Hz)	R (ohm/Mile)	L (mH/Mile)	G (μ -Mho/Mile)	C (μ F/Mile)
1	174.27	0.9861	0.000	0.083
5	174.27	0.9861	0.001	0.083
10	174.27	0.9861	0.001	0.083
15	174.27	0.9861	0.001	0.083
20	174.27	0.9861	0.002	0.083
30	174.27	0.9861	0.003	0.083
50	174.27	0.9861	0.005	0.083
70	174.27	0.9861	0.006	0.083
100	174.27	0.9861	0.009	0.083
150	174.27	0.9860	0.013	0.083
200	174.27	0.9860	0.017	0.083
300	174.28	0.9860	0.024	0.083
500	174.29	0.9858	0.040	0.083
700	174.29	0.9857	0.054	0.083
1,000	174.31	0.9856	0.076	0.083
1,500	174.34	0.9853	0.110	0.083
2,000	174.37	0.9850	0.145	0.083
3,000	174.44	0.9844	0.211	0.083

Frequency (Hz)	R (ohm/Mile)	L (mH/Mile)	G (μ -Mho/Mile)	C (μ F/Mile)
5,000	174.62	0.9833	0.341	0.083
7,000	174.83	0.9821	0.467	0.083
10,000	175.22	0.9804	0.652	0.083
15,000	176.06	0.9778	0.954	0.083
20,000	177.11	0.9744	1.248	0.083
30,000	179.86	0.9672	1.824	0.083
50,000	187.64	0.9491	2.943	0.083
70,000	197.71	0.9372	4.032	0.083
10,0000	215.55	0.9237	5.630	0.083
150,000	247.57	0.9055	8.229	0.083
200,000	277.95	0.8898	10.772	0.083
300,000	333.39	0.8642	15.744	0.083
500,000	421.57	0.8309	25.396	0.083
700,000	493.24	0.8123	34.796	0.083
1,000,000	583.59	0.7950	48.587	0.083
1,500,000	707.91	0.7783	71.014	0.083
2,000,000	812.72	0.7681	92.958	0.083
3,000,000	988.53	0.7557	135.865	0.083
5,000,000	1267.31	0.7429	219.158	0.083
7,000,000	1493.93	0.7367	300.284	0.083
10,000,000	1779.64	0.7309	419.297	0.083
15,000,000	2172.76	0.7254	612.834	0.083
20,000,000	2504.18	0.7222	802.205	0.083

Table A.2 24 AWG Characteristic at 70 Degrees F

Frequency (Hz)	R (ohm/Mile)	L (mH/Mile)	G (μ -Mho/Mile)	C (μ F/Mile)
1	277.19	0.9861	0.000	0.083
5	277.19	0.9861	0.001	0.083
10	277.19	0.9861	0.002	0.083
15	277.19	0.9861	0.003	0.083
20	277.19	0.9861	0.004	0.083
30	277.19	0.9861	0.005	0.083
50	277.19	0.9861	0.008	0.083
70	277.19	0.9861	0.011	0.083
100	277.19	0.9861	0.016	0.083
150	277.20	0.9860	0.022	0.083
200	277.20	0.9860	0.028	0.083
300	277.20	0.9860	0.040	0.083
500	277.21	0.9859	0.063	0.083
700	277.22	0.9858	0.084	0.083
1,000	277.23	0.9857	0.115	0.083
1,500	277.25	0.9854	0.164	0.083
2,000	277.28	0.9852	0.210	0.083
3,000	277.34	0.9848	0.299	0.083
5,000	277.48	0.9839	0.466	0.083
7,000	277.66	0.9829	0.625	0.083
10,000	277.96	0.9816	0.853	0.083
15,000	278.58	0.9793	1.213	0.083

Frequency (Hz)	R (ohm/Mile)	L (mH/Mile)	G (μ -Mho/Mile)	C (μ F/Mile)
20,000	279.35	0.9770	1.558	0.083
30,000	281.30	0.9723	2.217	0.083
50,000	286.82	0.9577	3.458	0.083
70,000	294.29	0.9464	4.634	0.083
10,0000	308.41	0.9347	6.320	0.083
150,000	337.22	0.9204	8.993	0.083
200,000	369.03	0.9087	11.550	0.083
300,000	431.55	0.8885	16.436	0.083
500,000	541.69	0.8570	25.633	0.083
700,000	632.08	0.8350	34.351	0.083
1,000,000	746.04	0.8146	46.849	0.083
1,500,000	902.84	0.7947	66.665	0.083
2,000,000	1035.03	0.7825	85.624	0.083
3,000,000	1256.77	0.7676	121.841	0.083
5,000,000	1608.38	0.7523	190.021	0.083
7,000,000	1894.20	0.7449	254.644	0.083
10,000,000	2254.56	0.7380	347.294	0.083
15,000,000	2750.38	0.7314	494.193	0.083
20,000,000	3168.38	0.7275	634.737	0.083

APPENDIX B.

B.1 Matlab's script features

This thesis is use Mathlab's software to simulate the transmission line characteristic and bridge taps effect. By writing the Matlab's script files, it use RLGC parameters of the telephone wire and the telephone loop length to simulate the Transfer function, Insertion Loss and SNR with downstream and upstream approximation. The Matlab's script file can support up to 10 bridge taps and support both 22 and 24 AWG. By using the parameter in Table 4.1. , it can simulate all the features that describe below:

- Power Spectral Density of Discrete Multitone ADSL (downstream and upstream).
- Power Spectral Density of NEXT (Near-End Crosstalk) and FEXT (Far-End Crosstalk).
- Transfer function of the transmission line.
- Characteristic Impedance of the transmission line.
- Insertion Loss.
- SNR (Signal-to-Noise Ratio) of both downstream and upstream.
- Downstream and Upstream data transfer rate approximation.

The RLGC parameters (Resistance, Inductance, Capacitance and Admittance) for both 22 and 24 AWG is in Appendix A.

APPENDIX C.

C.1 Component Price List

Table C.1 Component Price List

Component		Cost	
Item No.	Description	US Dollar / Unit	Baht / Unit
1	DSL Concentrator (Stinger)	2,865.50	118,860.94
2	ADSL Line Interface Module for 24 Ports	3,427.00	142,151.96
3	Stinger Trunk Module (DS-3)	1,008.25	41,822.21
4	ADSL Line Protection Module 48 Ports	302.00	12,526.96
5	DSL Terminator	3,166.45	131,344.35
6	DSL Terminator DS-3 Module	1,150.00	47,702.00
7	Cell Pipe 20A (ADSL Modem)	173.25	7,186.41
8	Rectifier for Stinger Module	3,730.00	154,720.40
9	Low Pass Filter	2.41	100.00
10	DSL-VSP (POTS Splitter)	27.25	1,130.33

Note: Exchange Rate is 1 US Dollar = 41.48 Baht

BIBLIOGRAPHY

- [1] ANSI/T1E1.4/94-007, Asymetric Digital Subscriber Line (ADSL) Metallic Interface Specification, September, 1994.
- [2] Aslanis J., and Cioffi J., "Achievable Information Rates on Digital Subscriber Loops: Limiting Information Rates with Crosstalk Noise," IEEE Transactions on Communications, vol. 40, no. 2, p. 361, February 1992.
- [3] Barton M., Chang L., and Hsing. R., "Performance of High-Speed Asymetric Digital Subscriber Lines Technology," IEEE Transactions on Communications, vol. 44, no. 2, p. 156, February 1996.
- [4] Brown R., "A Study of Local Loop Modem Limitations," AG Communication Systems, February 1998.
- [5] Chen W., "DSL Simulation Techniques and Standards Development for Subscriber Line Systems," Macmillan Technical Publishing, IN, March 1998.
- [6] Chen W., and Waring D., "ADSL Noise Environment and Potential System Performance," IEEE International Conference on, vol. 1, p. 451-455, 1994.
- [7] Chow P., Cioffi J., and Bingham J., "DMT-Based ADSL: Concept, Architecture, and Performance," IEE Colloquium on High speed Access Technology and Services, Including Video-on-Demand (Digest No. 1994/192), p. 3/1 -3/6, 1994.
- [8] Cioffi J., "Asymmetric Digital Subscriber Lines," CRC Press, p.450- 479, 1997.
- [9] Dutta-Roy A., "A Second Wind for Wiring," IEEE Spectrum. , p. 52-60, September, 1999.
- [10] Forney G., and Eyuboglu V., "Combined equalization and coding using precoding," IEEE Communication Magazine, vol. 29, no. 12, 1991.

- [11] Hoque M., "Radio frequency interference aspects of VDSL," ANSI T1E1.4/95-132, Orlando, FL, December, 1995.
- [12] Huang G., and Werner J.J., "Cable Characteristics," ANSI Contribution T1E1.4/97-169, Clearwater, FL, May 12, 1997.
- [13] Jackson A., "ADSL for High Speed Broadband Data Service," IEEE Aerospace Conference 1998, vol. 4, p. 451-465, 1998.
- [14] Kenneth K., "The range of baseband ADSLs as a function of bit rate," Global Telecommunications Conference, IEEE vol. 1, p. 40-44, 1992.
- [15] Kyees P., McConnell R., and Sistanizadeh K., "ADSL: A new Twisted-Pair Access to the Information Highway," IEEE Comm. Mag., April, 1995.
- [16] Lawrence R.W., "Impulse noise test results for 3 line-code technologies proposed for ADSL testing-preliminary report," ANSI T1E1.4/93-078, NYNEX, Miami, FL, March 10, 1993.
- [17] Lin S., and Costello D., "Error Control Coding: Fundamentals and Applications," Englewood Cliffs, NJ: Prentice Hall, 1983.
- [18] Manhire L., "Physical and Transmission Characteristics of Customer Loop Plant," Bell System Technical Journal 57, p. 35-39, January 1978.
- [19] Rauschmayer D., "ADSL/VDSL Principles," Macmillan Technical Publishing, IN, 1999.
- [20] Schwartz M., "Broadband Integrated Networks," Prentice Hall PTR, 1996.
- [21] Shannon C., "A mathematical theory of communication," BSTJ, 27, p. 379-423, 623-656, 1948.
- [22] Stevens R., "TCP/IP Illustrated, Volume 1 : The Protocols," Addison-Wesley Professional Computing Series, January 1994.

- [23] Waring D., "The Asymmetrical Digital Subscriber Line (ADSL: A New Transport Technology for Delivering Wideband Capabilities to the Residence," in Conf. Record GLOBECOM, Session 56.3, Phoenix, AZ, December. 1991.
- [24] Werner J.J., "The HDSL Environment," IEEE Journal on Selected Areas in Communications, vol. 9, no. 6, August 1991.
- [25] Zogakis N., Aslanis J., and Cioffi J., "A Coded and Shaped Discrete Multitone System," IEEE Transactions on Communications, vol. 43, no. 12, p. 2941, December 1995.
- [26] www.adsl.com



